1962

Radiochemical studies of some pile-neutron fission yields of thorium-232

James Matthew Crook
Iowa State University

RADIOCHEMICAL STUDIES OF SOME PILE-NEUTRON FISSION YIELDS OF THORIUM-232

by

James Matthew Crook

A Dissertation Submitted to the
Graduate Faculty in Partial Fulfillment of
The Requirements for the Degree of
DOCTOR OF PHILOSOPHY

Major Subject: Physical Chemistry

Approved:

Signature was redacted for privacy.

In Charge of Major Work

Signature was redacted for privacy.

Head of Major Department

Signature was redacted for privacy.

Dean of Graduate College

Iowa State University
Of Science and Technology
Ames, Iowa

1962

TABLE OF CONTENTS

I. INTRODUCTION

A. Review of the Literature

Following the discovery of the neutron in 1932, thorium and uranium were bombarded with neutrons in attempts to produce new isotopes, especially transuranic isotopes (98). A confusing abundance of activities were produced; they were generally considered to be members of the (4n + 1) series (32) and possibly transuranic (14). A difference between slow-neutron bombardment of thorium producing protoactinium-233 and fast-neutron bombardment producing protoactinium-233 and other activities was observed (62). These experiments culminated in the suggestion of fission in uranium (43); shortly thereafter, the neutron fission of uranium (33), and then thorium (23, 78), were confirmed. Other early experiments showed that thorium fission was asymmetric (42) with a cross section of about 10^{-25} cm.^{2} (52), and required fast neutrons (0.5- to 2.4-Mev.) (78).

Most work on thorium fission was temporarily postponed because of the emphasis on uranium-235 fission, but later interest revived because of general curiosity and the possible use of thorium as a breeder-conversion of abundant thorium-232, with its fast-neutron fission and low fission cross section, into the artificial isotope, uranium-233, with its slow-neutron fission and much larger fission cross section. Know-

ledge of the yields of the thorium fission products was needed to indicate such things as the required shielding, health hazards, decontamination problems, and poisoning of the fission reaction.

For more theoretical work, mass yields were needed to determine the mass distribution in fission and independent yields were needed to determine the charge distribution in fission. In either case, absolute yields were required to find the formation cross sections of particular mass chains or of particular isotopes. Since the direct measurement of absolute yields was difficult, in general, yields were determined relative to a reference mass number and the relative yield curve obtained was then normalized to 200 per cent to give absolute yields.

The main features of the mass distribution curve and, to a lesser extent, the charge distribution in fission require extensive rather than highly accurate data. The original data on uranium-235 (10) and thorium-232 (96), in general accurate to about $\pm$ 20 per cent, were adequate for these purposes. However, for fine structure greater accuracy was required, the largest deviation from the "smooth" yield curve being about 35 per cent for xenon isotopes in the thermal-neutron fission of uranium-235 (57).

The determination of mass yields required three main operations, gross separation, purification of a particular iso-

tope, and the determination of the number of atoms of this isotope.

The gross separation of an isotope has been done chemically, usually aided by the addition of a carrier (10). The noble gases, krypton and xenon, have been separated by boiling off, and again a carrier was usually added (87). A direct mass separation of iodine isotopes has also been used (8).

The purification of an isotope has been done chemically, through repeated cycles of chemical operations designed to reduce contamination by other fission products (10, 48, 61). Milking operations can give very pure isotopes. For example, barium can be separated rather pure from contamination except for radium, and lanthanum milked from this barium can be very free from contamination. Mass spectrographic methods require little purification because the method inherently discriminates against masses outside of the mass range of interest.

The determination of the number of atoms of a separated and purified isotope has been done with Geiger-Müller or four-pi proportional beta counters and with mass spectrometers.

The Geiger-Müller detectors have been by far the most commonly used. The recovery of the isotope through the separation and purification steps was usually found by weighing the recovered carrier. The Geiger-Müller method has two main advantages: it is extremely sensitive, easily capable of detecting 10^7 atoms of an isotope having a four day half-life;

and it is relatively easy to use, not requiring extensive equipment or elaborate techniques. Its main disadvantage is that large corrections are needed to convert the observed counts to the total number of atoms present. These include corrections for the efficiency, dead-time, and geometry of the detector, corrections for the loss of activity due to absorption in the sample, sample covering, intervening air, and the window of the detector, and corrections due to fore- and back-scattering (106). A common device to circumvent these corrections has been to measure the activity of a particular isotope from the fission of some fissile material relative to the activity of the same isotope from the thermal-neutron fission of uranium-235; hence, the result was the yield in the fissile material relative to the yield in uranium-235 (96). Although the results could be no better than the uranium-235 yields, this technique permitted the use of data from the enormous amount of work done on uranium-235 yields.

The Geiger-Müller method does not directly determine the mass number or atomic number of the detected activity, but because of the extensive work that has been done on many isotopes (84), there is usually little doubt as to which isotope is being counted. This method of determining the activity of a particular isotope may be complicated by the presence of daughter and isotopic activities. Of course, this method cannot be used to detect stable isotopes.

Mass spectrometric methods eliminate many of the corrections involved in Geiger-Müller counting. The main advantages are the direct assignment of mass numbers and the detection of stable isotopes (86). The use of isotopic dilution techniques (40) has given relative yields of some isotopes with an accuracy of perhaps $\pm$ 1 per cent (87). This accuracy resulted in the discovery of fine structure in the mass yield curve of uranium-235 (57). Mass spectrometric methods need more elaborate equipment and are not as sensitive as the Geiger-Müller method, requiring in the case of krypton-85 a minimum of 10^{11} atoms (86).

Four-pi proportional counters have also been used to determine fission yields (2). This method has many of the features of the Geiger-Müller method. The main advantage is the elimination of many of the corrections required in the Geiger-Müller method; corrections for self-absorption and absorption in the sample support film, while difficult to determine accurately, can be very small under suitable conditions. This method requires more sensitive determinations of recovered carriers as smaller amounts of carriers are added in order to increase the specific activity of the counting sample; usually spectrophotometric determinations are used.

B. Purpose of the Investigation

The purpose of this work was to determine improved relative yields of some masses produced in the pile-neutron

fission of thorium-232 using the four-pi proportional beta counter technique. Published separation procedures were modified to provide the increased specific activities required for the four-pi counting and to remove the large amounts of protoactinium-233 contamination produced by neutron capture in pile-neutron irradiation of thorium. Purified lanthanum and yttrium activities were obtained from their respective parents, barium and strontium, by milking methods after these parents had been separated from other fission products. Yttrium and rare earth activities were separated from other fission products by ion-exchange methods. The recoveries of the carriers after separation and purification steps were determined spectrophotometrically.

II. EXPERIMENTAL METHODS

A. Materials

The thorium metal, yttrium, lanthanum and the rare earths praseodymium and neodymium used in the experiments were produced at the Ames Laboratory. The thorium was in the form of a foil, approximately five mils thick.. The reagent 3-(2-arsonophenylazo)-4,5-dihydroxy-2,7-naphthalene-disulfonic acid trisodium salt · $2H_2O$, "arsenazo", was provided by C. V. Banks of the Ames Laboratory.

Tygon paint and tygon thinner were obtained from the U. S. Stoneware Company, Akron, Ohio.

B. Equipment

1. Four-pi proportional counter

A four-pi proportional counter, model CE-10 (Tracerlab Inc., Boston, Massachusetts) was used to measure the absolute disintegration rates of various isotopes. The manufacturer stated that the resolving time of the counter, with its associated preamplifiers, was less than 1.0 microseconds; it was determined to be less than 2 microseconds.

The scaling unit used with the four-pi counter was an Ampliscaler, model SC-32ES (Tracerlab Inc.). The manufacturer stated that the resolving time of the scaler was 5 microseconds, permitting counting rates up to 120,000 counts/minute

with less than 1 per cent coincidence loss. The scaler was modified by the manufacturer for use with the four-pi counter and counting measurements could be taken on either counting chamber or both chambers together (in parallel).

A separate power supply was used to provide high voltage to the counter anodes. The anode voltage could be varied from 0 to 5000 volts.

Methane gas, C. P., 99 per cent (Phillips Petroleum Company, Bartlesville, Oklahoma) was used as the counter flow gas.

2. General counting equipment

Standard end window, self-quenching Geiger-Müller counting tubes were used for routine beta counting. These tubes were used with standard lead housings and scalers. An "Ametron" counter (Streeter-Amet Company, Chicago, Illinois) was used on occasion to record total counts at intervals of 4 to 60 minutes.

3. Gamma-spectrometer

A 256 Channel Analyzer (Radiation Counter Laboratories, Inc., Skokie, Illinois) was used to measure the gamma spectra of various isotopes.

4. Spectrophotometers

Two Beckman model DU spectrophotometers (Beckman Instruments, Inc., Fullerton, California) were used; one had a photomultiplier detector, the other a photocell detector.

One-centimeter, glass stoppered or ground-glass stoppered, Corex cells were used. No attempt was made to control the temperature of the cell compartments or to calibrate the wave-lengths used; a standard curve of absorbance versus concentration was redetermined with each set of unknowns run.

5. pH meter

A Beckman model "G" pH meter was used to measure pH's when required. External, shielded electrodes, Beckman model 1190-80, were used. The instrument was calibrated with pH 4 or pH 7 buffers.

6. Vacuum evaporator

A Vacuum Unit, Type EMV-1A, (Radio Corporation of America, Camden, New Jersey) was used to evaporate aluminum onto four-pi sample films.

7. Micropipets

Micropipets, usually of 50 or 100 lambda capacity, were used to take aliquots of various solutions for counting samples and spectrophotometric analyses. Initially the pipets were desicoated to permit use as volumetric "to contain" pipets (15), calibrating by weighing pipetted mercury or by titrating pipetted 11 N. $HClO_4$ with 0.02 N. NaOH. However, the desicoated pipets were difficult to clean and to keep clean, so non-desicoated pipets were used as volumetric "to deliver" pipets. Since only the ratio between the counting sample and the spectrophotometric analysis sample was needed,

the same pipet was used for both samples, making knowledge of the exact volume delivered unnecessary. The pipets were cleaned with alkaline permanganate solution, rinsed with saturated oxalic acid solution, rinsed with hot water, and dried with a stream of filtered air. The pipets were cleaned several hours before use.

8. Ion-exchange column

An ion-exchange column was used to separate the rare earth fission products. The column was maintained at an operating temperature of about 87 °C. by means of a water-bath jacket. The reservoir section above the resin was heated to about 105 °C. in order to pre-heat the eluant. During operation the top of the resin column was about 2 °C. warmer than the bottom.

C. Irradiation

Samples of about three grams of thorium foil, sealed in a quartz vial, were irradiated in the CP-5 reactor of the Argonne National Laboratory, Lemont, Illinois. The irradiations occurred in the "VT" locations of the reactor; these locations made use of an enriched-in-uranium-235 uranium sleeve in order to convert part of the slow neutrons into fast neutrons, thus increasing the relative number of fast neutrons at these locations. Descriptions of the CP-5 reactor have been published (60, 105).

The thorium samples were irradiated for about one day at fluxes of the order of 10^{13} neutrons/square centimeter/second. The fast neutron flux to slow neutron flux ratio was about two. The flux was not under my control so the yields determined in one irradiation were related to the yields determined in another irradiation by determining a reference yield.

D. Solution of Thorium

Thorium metal was dissolved in concentrated hydrochloric acid to which sufficient $(NH_4)_2SiF_6$ solution was added to make it approximately 0.1 M. in $SiF_6^=$ following the procedure of Newton, Hyde, and Meinke (61, p. 195). A small amount of a blue-black residue was always present after solution. The solution of non-irradiated thorium was complete (except for the residue) in less than thirty minutes; addition of more HCl-$SiF_6^=$ solution or heating did not appear to decrease the amount of residue. Irradiated thorium dissolved more slowly than non-irradiated thorium; the solution was aided by heating in a hot water bath or by leaving the solution overnight before further chemistry. A polyethylene beaker was used for the dissolution in order to prevent any adsorption or "plating-out" of the carrier-free fission products on the walls of glass vessels.

The procedure was as follows:

a. The aluminum can with the irradiated thorium sample was removed from its shipping container, surveyed for radioactivity, and placed behind a four inch lead brick barrier in a stainless steel hood.

b. The aluminum can was cut away and the quartz vial containing the thorium sample was placed in a long lusteroid tube. The lusteroid tube was sealed with two inch plastic tape, then placed in a clamping arrangement. A thumbscrew was tightened in the clamp to break the vial. The lusteroid tube was cut open and the thorium transferred to a 200 ml. polyethylene beaker.

c. About 5 ml. of concentrated HCl (approximately 0.1 M. in $SiF_6^{=}$) were added and the beaker covered with a watch glass. After an induction period of 15-30 seconds, the reaction was vigorous. (In dissolving later thorium samples, a large beaker, inverted, was used as an additional cover. This reduced the contamination of the hood from "spray" markedly. This beaker was not necessary after the first vigorous reaction.)

d. About 15 ml. of the HCl-$SiF_6^{=}$ solution were added in 5 ml. portions at intervals of 10-20 minutes.

e. The thorium solution was either left overnight or placed in a hot water bath (not boiling). When

solution was complete, about 80 ml. of water were added.

f. Appropriate samples were taken in centrifuge tubes containing solutions of the desired carriers.

E. Radiochemical Separations

1. Mass number 140

The yield of mass number 140 was determined by separating barium-140 from other fission products. After the separation of barium, the lanthanum-140 daughter of barium-140 was allowed to grow to secular equilibrium. The lanthanum was then removed as described below and used to determine the barium-140. This process of removing a daughter product in equilibrium with its parent as a method of determining the parent activity, known as milking, was used frequently in these separations.

The barium separation of Newton (61, p. 179) was closely followed except that zirconium was used as a scavenger in addition to iron and two such scavenges were made. Briefly, the barium was precipitated as the sulfate, converted to the carbonate, precipitated twice as the nitrate with fuming nitric acid, scavenged twice with iron and zirconium by the addition of gaseous ammonia, precipitated as the chromate from a buffered solution, and precipitated twice as the chloride from a HCl-ether solution. The final barium chloride pre-

cipitate was filtered on a weighed filter-disk in a sintered-glass filter-stick, dried in a vacuum, and weighed as $BaCl_2 \cdot H_2O$.

The barium was precipitated as the sulfate prior to the removal (scavenge) of protoactinium by coprecipitation on zirconium iodate for two reasons: (a) when cerium was also present, it was added as a sulfate solution, and (b) if barium were present when zirconium was precipitated as the iodate, some barium would be lost in the form of a barium-zirconium-iodate precipitate.

After the barium separation, lanthanum-140 was milked from the barium-140:

a. The barium chloride was dissolved in 10 ml. of 0.1 N. HCl and 1 mg. of lanthanum in the form of a lanthanum chloride solution was added. Lanthanum was precipitated with gaseous ammonia.

b. The lanthanum precipitate was dissolved in 6 drops of 6 N. HCl. One mg. of barium in the form of a barium chloride solution and 4 ml. of water were added and lanthanum was precipitated with gaseous ammonia.

c. Step b was repeated and the lanthanum precipitate was washed with 4 ml. of water.

d. The lanthanum precipitate was dissolved in 2 drops of 6 N. HCl. Water was added to bring the solution to

a suitable volume (usually about 1 ml.).

e. Samples were taken for counting and spectrophotometric analysis.

2. Mass number 89

The yield of mass number 89 was determined by separating and counting strontium-89. The separation of Newton (61, p. 107) was closely followed except that zirconium was used as a scavenger in addition to iron and two such scavenges were made. Briefly, the strontium was precipitated as the sulfate, converted to the carbonate, precipitated twice as the nitrate with fuming nitric acid, scavenged twice with iron and zirconium by the addition of gaseous ammonia, separated from barium by precipitating barium chromate from a buffered solution, and precipitated as the oxalate. The strontium oxalate precipitate was filtered on a weighed filter-disk in a sintered-glass filter-stick, dried in a vacuum, and weighed as $SrC_2O_4 \cdot H_2O$. The strontium oxalate was dissolved and diluted to a known volume and aliquots were taken for counting.

3. Mass number 90

The yield of mass number 90 was determined by separating strontium-90. After the strontium separation, the yttrium-90 daughter of strontium-90 was milked and counted. The strontium separation was as given for mass number 89. The procedure for milking yttrium-90 from strontium-90 was the

same as that given for the milking of lanthanum-140 from barium-140 with yttrium and strontium in the place of lanthanum and barium respectively. The strontium oxalate precipitate was dissolved and diluted to a known volume and aliquots were taken for milking.

4. Mass number 91

The yield of mass number 91 was determined by separating and counting yttrium-91. The separation procedure was the same as used for mass number 141, through the preliminary and ion-exchange separations. The final separation was the same with yttrium in the place of cerium except for Step 4 which was replaced as follows:

4. To the yttrium solution were added one-half mg. of cerium carrier and one-fourth gram of $KBrO_3$ to precipitate cerium (IV) iodate. The yttrium solution was transferred to a 12 ml. centrifuge tube.

5. Mass number 99

The yield of mass number 99 was determined by separating and counting molybdenum-99. The molybdenum separation procedure was adapted from the procedures of Hiller (37) and Newton (61, p. 117), scaled down to separate 2 mg. of molybdenum carrier, with additional steps to ensure removal of protoactinium-233, and modified to use separatory tubes instead of separatory funnels in the ether extraction of

molybdenum.

The separatory tubes were large test tubes plus hollow glass "T" stirrers. A small hole was blown in the stem of the "T", situated so that the hole was in the upper phase during operation. When the "T" stirrer was turned on, a pumping action resulted which thoroughly mixed the two phases. After settling, the upper phase was withdrawn by means of a needle-nose eyedropper. This extraction procedure was much easier to use with the radioactive samples than the regular procedure using separatory funnels. The procedure was as follows:

a. The thorium solution was pipetted into a 40 ml. centrifuge tube and 2 mg. of molybdenum carrier, 1 mg. of zirconium carrier, and 4 drops of bromine were added. The bromine was boiled off.

b. The solution was transferred to separatory tubes, made 6 N. in HCl, and extracted three times with 6 ml. of HCl-saturated ether.

c. The combined ether phases were washed twice with 3 ml. of 6 N. HCl, then evaporated over 2 ml. of water with a stream of air, using heat to boil off the last traces of ether.

d. The molybdenum residue was transferred to a 5 ml. centrifuge tube using 1 ml. of 6 N. HNO_3, one-fourth ml. of saturated oxalic acid, and 1 ml. of

water. One ml. of fresh alpha-benzoinoxime (in 95 per cent ethanol) was added to precipitate molybdenum. The molybdenum precipitate was washed with 3 ml. of 1 N. HNO_3.

e. The precipitate was dissolved in one-half ml. of 6 N. NaOH. The solution was acidified with concentrated HNO_3, then 1 ml. of the alpha-benzoinoxime reagent was added. The molybdenum precipitate was transferred to a 30 ml. beaker using 2 ml. of concentrated HNO_3.

f. The sample was evaporated to near-dryness with a flame. One ml. of concentrated HNO_3 and one-half ml. of concentrated $HClO_4$ were added and the heating repeated.

g. The molybdenum residue was dissolved with 2 ml. of water and one-half ml. of concentrated NH_4OH. The solution was transferred to a 5 ml. centrifuge tube and acidified with 6 N. HNO_3. One mg. of zirconium carrier and 1 ml. of ferric carrier were added and the hydroxides precipitated with one-half ml. of concentrated NH_4OH.

h. The supernatant liquid was decanted into a 5 ml. centrifuge tube and acidified with concentrated HNO_3. Molybdenum was precipitated with 2 ml. of the alpha-benzoinoxime reagent, washed with 3 ml. of 1 N. HNO_3,

and transferred to a 30 ml. beaker by slurrying with 2 ml. of concentrated HNO_3. One ml. of concentrated $HClO_4$ was added and the mixture gently evaporated to near-dryness with a flame.

i. The molybdenum residue was dissolved in 1 ml. of water and 2 ml. of concentrated NH_4OH.

j. Samples were taken for counting and spectrophotometric analysis.

6. Mass number 141

The yield of mass number 141 was determined by separating and counting cerium-141. A cerium separation was attempted using essentially the procedures of Ames (48) or Newton (61, p. 195). These involved a separation of cerium (III) from the gross fission products by a fluoride precipitation, separation of cerium (III) from protoactinium-233 by a zirconium iodate scavenge, and separation of cerium from other rare earths by a cerium (IV) iodate precipitation. However, the recovery of 1-2 mg. of the cerium carrier was too low to be of value. Hence the cerium was separated by means of an ion-exchange method.

A preliminary separation from the gross fission products, involving a fluoride precipitation followed by a zirconium iodate scavenging, preceded the column separation. After elution, the appropriate fractions were combined and the lactic acid destroyed by perchloric oxidation. Gamma spectra

run on the 256 Channel Analyzer Gamma-Ray Spectrometer indicated the presence of protoactinium-233, so the separated rare earths were purified by zirconium iodate scavenges.

a. Preliminary separation The preliminary fluoride precipitation and zirconium scavenging was done as follows:

1. About 1 mg. each of cerium, praseodymium, neodymium, samarium, yttrium, and lanthanum in the form of carrier solutions were added to a thorium solution.
2. After a barium sulfate precipitation, 2 ml. of concentrated HF were added. The rare earth fluoride precipitate was washed with 10 ml. of 1 N. HCl, washed with 10 ml. of water, and dissolved in 8 ml. of concentrated nitric acid plus 1 ml. of saturated boric acid solution.
3. To the solution, 2 drops of 30 per cent hydrogen peroxide and 3 ml. of fresh 3.5 M. HIO_3 were added to precipitate zirconium iodate.
4. To the supernatant liquid, 19 N. sodium hydroxide was added until the solution was basic, precipitating the rare earth hydroxides. The hydroxides were washed with 10 ml. of water, then dissolved in 1 ml. of 6 N. HCl plus 1 drop of sulfurous acid.
5. The rare earth hydroxides were precipitated with 6 N. ammonium hydroxide, washed with 5 ml. of water, and dissolved in 5 drops of 6 N. HCl.

6. The final solution was transferred to a Dowex-50W ion-exchange column.

b. Ion-exchange separation The ion-exchange separation was based on the procedures of several authors (13, 24, 59). The column used Dowex-50W in the NH_4^+ form with 1 M. lactic acid at a pH of 3.22 as the eluant. The column was operated at a temperature of about 87 °C. and the eluant was pre-heated to about 105 °C. Five minute samples were collected in small plastic planchets, beginning 20 minutes after the rare earths were transferred to the column. The elution rate was adjusted to 11 to 14 seconds per drop, equivalent to 10 to 8 ml. per hour, for samples #1 to #144. Then the elution rate was increased to about 6 seconds per drop through sample #287. The course of the elution was followed by counting the samples as they were removed from the column. The gamma-ray spectra of the samples not only showed the presence of protoactinium-233, but also clearly indicated the cerium and lanthanum peaks.

c. Final separation The final separation to remove the lactic acid and protoactinium-233 was done as follows:

1. The samples comprising the cerium elution peak were combined by transferring the eluted material from the planchets to a 250 ml. erlenmeyer flask using 0.1 N. HCl.
2. The volume was reduced by evaporating to near-dryness

on a hot plate. The lactic acid present was removed by heating to near-dryness on a hot plate three times with 10 ml. of concentrated HNO_3, once with 5 ml. of concentrated HNO_3 plus 5 ml. of concentrated $HClO_4$, and twice with 1 ml. of concentrated HNO_3 plus 10 ml. of concentrated $HClO_4$.

3. The cerium residue was dissolved in 2 ml. of concentrated HNO_3 and transferred to a 12 ml. centrifuge tube. To the cerium solution were added 1 mg. of zirconium carrier and 6 drops of fresh 3.5 M. HIO_3, forming a zirconium iodate precipitate. The cerium solution was transferred to a 12 ml. centrifuge tube.
4. To the cerium solution were added one-half mg. of lanthanum carrier and one-fourth gram of $KBrO_3$, forming a cerium iodate precipitate. The cerium iodate was dissolved in 4 drops of 6 N. HCl, 1 drop of 30 per cent H_2O_2, and 3 ml. of concentrated HNO_3.
5. To the cerium solution was added 19 N. NaOH until the solution was basic, precipitating the hydroxide. The precipitate was washed with 4 ml. of water, then dissolved in 4 drops of 6 N. HCl and 2 drops of sulfurous acid.
6. The cerium hydroxide was reprecipitated with 1 ml. of concentrated NH_4OH, washed with 4 ml. of water,

and dissolved in 1 drop of 6 N. HCl. Water was added to bring the solution to a suitable volume, usually 1 ml.

7. Samples were taken for counting and spectrophotometric analysis.

7. Mass number 143

The yield of mass number 143 was determined by separating and counting praseodymium-143. The separation procedure was the same as used for mass number 141 through the preliminary and ion-exchange separations. The final separation was the same with praseodymium in the place of cerium except for Step 4 which was replaced as follows:

4. To the praseodymium solution were added one-half mg. of cerium carrier and one-fourth gram of $KBrO_3$ to precipitate cerium(IV) iodate. The praseodymium solution was transferred to a 12 ml. centrifuge tube.

8. Mass number 144

The yield of mass number 144 was determined by separating and counting cerium-144. The cerium separation for mass number 141 was used.

The praseodymium-144 daughter of cerium-144 was milked and counted to confirm the presence of cerium-144. Because of the short half-life of praseodymium-144, only an estimate of the parent cerium-144 activity could be made by milking. Praseodymium was milked from cerium by precipitating

cerium(IV) as the iodate:

a. One mg. of praseodymium carrier was added to 10 ml. of cerium solution. The cerium and praseodymium were precipitated with 2 ml. of 19 N. NaOH, and washed with 3 ml. of water.

b. The hydroxides were dissolved in 2 ml. of concentrated HNO_3. One-fourth gram of $KBrO_3$ was added. Cerium iodate was precipitated with 6 drops of fresh 3.5 M. HIO_3. The supernatant liquid was transferred to a clean tube.

c. One-half mg. of cerium(III) carrier was added to the supernatant liquid and the cerium iodate precipitated. One-fourth gram of $KBrO_3$, 1 mg. of zirconium carrier, and 6 drops of 3.5 M. HIO_3 were added and the zirconium iodate precipitated. The supernatant liquid was transferred to a clean tube.

d. To the supernatant liquid, 19 N. NaOH was added dropwise until the solution was basic, precipitating praseodymium hydroxide. The precipitate was washed with 3 ml. of water and dissolved in 3 drops of 6 N. HCl.

e. All of the final solution was used as a counting sample.

9. Mass number 147

The yield of mass number 147 was determined by separating and counting neodymium-147. The separation procedure was the

same as used for mass number 141 through the preliminary and ion-exchange separations. The final separation was the same with neodymium in the place of cerium except for Step 4 which was replaced as follows:

4. To the neodymium solution were added one-half mg. of cerium carrier and one-fourth gram of $KBrO_3$ to precipitate cerium(IV) iodate. The neodymium solution was transferred to a 12 ml. centrifuge tube.

F. Spectrophotometric Determinations

1. Molybdenum

The determination of molybdenum was made by a homogeneous acetone thiocyanate method developed by Crouthamel and Johnson (12). In their procedure, molybdenum(VI) was reduced to molybdenum(V) in 4 M. HCl with fresh cuprous chloride (in concentrated HCl). The molybdenum(V)-thiocyanate color was developed by adding 1 M. ammonium thiocyanate solution (in acetone). The procedure used was as follows:

a. The molybdenum samples were pipetted into 25 ml. volumetric flasks and 2 ml. of 8 N. HCl were added. Suitable standards were prepared with a molybdenum standard solution (99.6 μg. molybdenum/ml.); 0.10 to 1.00 ml. of the standard solution were buretted into 25 ml. volumetric flasks and 8 N. HCl was added to give a total volume of 2 ml.

b. Fresh cuprous chloride (in concentrated HCl) was prepared and 5 drops were added to the molybdenum solutions. About 10 ml. of water were added.

c. To groups of three samples were added 15 ml. of fresh 1 M. ammonium thiocyanate solution (in acetone). Sufficient water was added to bring the total volume to about 25 ml.

d. Fresh cuprous chloride (in concentrated HCl) was prepared and 5 drops were added. The solutions were diluted to 25 ml. with water.

e. The molybdenum(V)-thiocyanate color developed at once and was measured at 460 mμ with a Beckman model DU spectrophotometer using one-centimeter ground-glass-stoppered corex cells.

The colors were measured within 20 to 30 minutes after the addition of ammonium thiocyanate. The ammonium thiocyanate was purified by recrystallizing from methanol; the 1 M. solution in acetone was prepared just prior to a complete run of standards and unknowns. The cuprous chloride solution was prepared immediately prior to each use.

2. Rare earth group -- cerium, praseodymium, neodymium, lanthanum and yttrium

The determination of the rare earth group involved the use of "arsenazo"--3-(2-arsonophenylazo)-4,5-dihydroxy-2,7-naphthalene-disulfonic acid trisodium salt · $2H_2O$. Two

similar methods were used with satisfactory results:

a. The first method was adapted from one developed by Fritz and coworkers at the Ames Laboratory (25).

1. Aliquots of a rare earth sample were pipetted into 50 ml. beakers. About 20 ml. of 0.01 N. HCl were added. Suitable standards were prepared with the appropriate rare earth standard solution; usually standards were prepared to cover the range of 0 to 200 μg. total rare earth. To the standard solutions, 0.01 N. HCl and water were added to give total volumes of about 20 ml. with similar acidic strength. (The addition of 0.01 N. HCl was not necessary but served to make the adjusting of the final solution pH's in Step 4 easier and faster.)
2. To the solutions, 2.00 ml. of arsenazo solution (about 1 mg. of arsenazo/ml.) were added. (On occasion, 3.00 ml. of arsenazo solution were added to cover a greater range.)
3. To the solutions, 5.0 ml. of 2 M. $NaNO_3$ were added.
4. The solution pH's were adjusted to 8.0 $\pm$ 0.1 with a Beckman model G pH meter using an external electrode. Dilute NH_4OH of approximately 0.1 N. and 0.01 N. and dilute HNO_3 of approximately 0.01 N. were used to adjust the pH.
5. The solutions were transferred to 50 ml. volumetric

flasks using very dilute NH_4OH solution (pH 8) to wash the beakers and to dilute the final solutions to mark.

6. The rare earth arsenazo colors were measured at 570 mμ with a Beckman model DU spectrophotometer using one-centimeter corex cells.

b. The second method was taken from one developed by Banks and coworkers (3).

1. This step was the same as Step 1 of Method a.
2. To the solutions, 5.00 ml. of arsenazo reagent (about 1.5 mg. of arsenazo/ml.) were added.
3. To the solutions, 5.00 ml. of a sodium-borate solution (pH 7.0 $\pm$ 0.1) were added.
4. This step was the same as Step 4 of Method a except that the final solution pH's were adjusted to 7.0 $\pm$ 0.1.
5. This step was the same as Step 5 of Method a except that water was used to transfer and to dilute the solutions to mark.
6. This step was the same as Step 6 of Method a.

The arsenazo reagent solution was prepared shortly before use; its concentration varied from one run to the next but the same solution was used for any one run of standards and unknowns.

G. Counting Procedures

Both beta and gamma counting were used in these experiments.

1. Geiger-Müller beta counting

G.-M. beta counting was used to determine the half-lives and, by means of aluminum absorbers, the maximum beta-ray energies of the various activities. Because of the chemical separations, there was little doubt of the activity being counted, and measured half-lives and beta-ray energies were used more as confirmation than as identification of the activity. The primary purpose of the G.-M. counting was to check the absence of contaminating activities, especially protoactinium-233. It was found that the lanthanum-140, milked from barium-140, yttrium-90, milked from strontium-90, molybdenum-99, and strontium-89 were free of contamination.

The G.-M. counting methods were those routinely used. Several G.-M. detector tubes, housings, and scalers were used, but the same system was used during any one determination. The counter dead-time corrections were determined by following the decay of a sodium-24 sample, by use of paired-samples of uranium (5), and by use of multiple paired-samples of uranium or mercury-203 (50). The counting rates seldom exceeded 10,000 counts per minute so that the dead-time corrections seldom exceeded five per cent. Measured half-lives and beta-ray energies are given and compared with literature

values in Section III A.

2. Gamma counting

Gamma counting was used to identify or to confirm the identity of the counted activity and to check the absence of contaminating activities, especially protoactinium-233. A 256 Channel Analyzer Gamma-Ray Spectrometer (83) was used. It was found that the yttrium-91, cerium-141, 144, praseodymium-143, and neodyminium-147 activities were free of contamination. The instrument was calibrated with beryllium-7, cesium-137, and mercury-203 samples. Observed gamma-rays are compared with literature values in Section III A.

3. Four-pi beta counting

Four-pi beta counting was used to determine the disintegration rates of the samples. The samples, on thin aluminum-coated plastic films, were counted between two two-pi proportional counters which were connected in parallel. The operation of the counter was checked with an uranium sample.

The observed counting rate was corrected for the background. The background varied from 120 to 250 counts per minute, but was constant over the course of any one experiment. As the sample counting rate was usually about 40,000 counts per minute, the background was only a small correction.

The corrections for self-absorption were not determined. They were minimized by using very small counting samples,

50 or 100 microliters, which were freeze-dried in a vacuum in order to keep the material spread out. The self-absorption corrections are discussed in Section III B 2.

The corrections for absorption in the aluminum-coated plastic films were not determined, but because the coated films had densities of about 20 μg./cm.^{2}, these corrections were negligible (64, 73). The corrections for absorption in the aluminum supports for the plastic films were not determined, but were negligible because the counting samples were placed over a 2.6 centimeter hole in the supports and the supports were only about one millimeter in thickness (64, 73). A description of the plastic films, the aluminum coating and the aluminum supports is given in Section V B.

The corrections for the 5 microseconds resolving time of the scaler usually amounted to about 0.3 per cent or less and were neglected except in one case where a correction of 1.3 per cent was used.

III. EXPERIMENTAL DATA AND RESULTS

The experimental results are given in two sections. In Section A pertinent data and calculated results are given for each mass number. The equations used are found in Section V A. The final fission yields are in the form

$$y_n = \frac{R_n}{K_x} ,$$

where y_n = the fission yield for mass number n,

K_x = a constant for thorium sample x

and R_n = the saturation disintegration rate of mass number n.

The observed net counting rate was converted to a disintegration rate by using $n_t = \frac{n_o}{1 - f_\beta}$, where n_t and n_o are the true disintegration rate and the observed net counting rate respectively and f_β is the self-absorption correction given in Section B.

In the tables, the following expressions are used:

T_o = the duration of the irradiation;

T_s = the time between the end of the irradiation and the separation of nuclide B from nuclide A;

T_2 = the time between the separation and counting of nuclide B;

T_m = the time between the separation of nuclide B and the milking of nuclide C;

T_3 = the time between the milking and counting of nuclide C;

$$\text{counting factor} = \frac{\text{sample counted}}{\text{sample carrier}} .$$

Also, these expressions are used in the case of the 140 mass chain (for example):

$(\text{La-140})_c$ = the activity at the time of counting;

$(\text{Ba-140})_s$ = the activity at the time of separation;

La-140 = the activity of the lanthanum counting sample;

$(\lambda_{La}N_{La})$ = the activity of the total lanthanum.

The expression $(\lambda_{La}N_{La})$ is used in place of $(\lambda_{La140}N_{La140})$ since the isotope in question is obvious.

In Section B the yields, y_n, the relative yields, $\frac{y_n}{y_{140}}$, and the absolute yields (y_{140} = 6.2 per cent) (45) are given along with a discussion of errors.

A. Data and Calculated Results

1. Mass number 140

Barium-140 was used to determine the fission yield of mass number 140. The barium-140 activity was found by milking and counting its daughter, lanthanum-140. The identification of the lanthanum was confirmed by measuring the half-life of the lanthanum activity and by estimating its beta-ray ranges in aluminum. These ranges were converted to maximum beta-ray energies (27); while not precise, these energies were compatible with beta-ray energies for lanthanum-140 (84).

Barium and lanthanum corresponded to nuclides B and C

respectively in the equations of Section V A, and half-lives of 12.8 days and 40.2 hours respectively (84) were used. The self-absorption correction, f_β, was 0.01.

a. Thorium sample 1 The observed half-lives of two lanthanum samples were 40.7 and 40.4 hours. A least-squares determination of the half-life, using twenty-four points having counting rates ranging from 5924 to 79 counts per minute, gave an observed half-life of 40.25 hours. The data and results are given in Table 1. The yield of mass number 140 was

$$Y_{140} = \frac{5.45 \times 10^7}{K_1} \text{ disintegrations per second.}$$

b. Thorium sample 2 The observed half-life of lanthanum was 39.8 hours. The data and results are given in Table 2. The yield of mass number 140 was

$$Y_{140} = \frac{8.8 \times 10^7}{K_2} \text{ disintegrations per second.}$$

2. Mass number 89

Strontium-89 was used to determine the fission yield of mass number 89. The counting sample also contained some strontium-90 and yttrium-90 activity. Aliquots of the separated strontium were milked with yttrium to determine the yttrium-90 present; from this the activity of the strontium-90-yttrium-90 pair was calculated to be 3.4 per cent of the total activity at the time of counting. The identity of the

Table 1. Experimental data and calculated results: mass number 140 -- thorium sample 1

Ba carrier (mg Ba)	36.06	36.06	
Ba recovered (mg $BaCl_2 \cdot H_2O$)	26.1	38.1	
La carrier (mg La)	2.48	2.48	
La counted (mg La)	0.178	0.152	0.152
$(La\text{-}140)_c$ (c/m - background)	30,250	34,370	35,420
$(La\text{-}140)_c$ (c/s)	504	573	590
$(La\text{-}140)_c$ (d/s)	509	579	596
La counting factor	0.072	0.061	0.061
$(\lambda_{La}N_{La})_c$ (d/s)	7070	9500	9770
T_3 (hours)	200.95	204.6	202.5
T_m (hours)	524.5	524.5	524.5
$(Ba\text{-}140)_s$ (d/s) (Equation 7)	6.42×10^5	9.25×10^5	9.14×10^5
$(Ba\text{-}140)_s$ (d/s) (ave.)	6.42×10^5	9.20×10^5	
Ba recovery (%)	44.0	64.1	
$(\lambda_{Ba}N_{Ba})_s$ (d/s)	1.44×10^6	1.42×10^6	
$(\lambda_{Ba}N_{Ba})_s$ (d/s) (ave.)	1.43×10^6		
T_s (days)	12.68		
T_o (days)	1.0		
Y_{140} (d/s) (Equation 3)	$\frac{5.45 \times 10^7}{K_1}$		

Table 2. Experimental data and calculated results: mass number 140 -- thorium sample 2

Ba carrier (mg Ba)		90.15	
Ba recovered (mg $BaCl_2 \cdot H_2O$)		5.1	
La carrier (mg La)		1.24	
La counted (mg La)	0.0342		0.0342
$(La\text{-}140)_c$ (c/m - background)	1123		1171
$(La\text{-}140)_c$ (c/s)	18.7		19.8
$(La\text{-}140)_c$ (d/s)	18.9		20.0
La counting factor	0.0276		0.0276
$(\lambda_{La}N_{La})_c$ (d/s)	684		724
T_3 (hours)	27.47		24.37
T_m (hours)	546		546
$(Ba\text{-}140)_s$ (d/s) (Equation 7)	3.50×10^3		3.51×10^3
$(Ba\text{-}140)_s$ (d/s) (ave.)		3.50×10^3	
Ba recovery (%)		3.4	
$(\lambda_{Ba}N_{Ba})_s$ (d/s)		1.03×10^5	
T_s (days)		71.84	
T_o (days)		1.083	
y_{140} (d/s) (Equation 3)		$\frac{8.8 \times 10^7}{K_2}$	

strontium-89 was confirmed by observing its half-life after correcting for the strontium-90 and yttrium-90 present. The range of the strontium activity in aluminum, without correcting for the strontium-90 and yttrium-90, gave an estimate of the maximum beta-ray energy compatible with that of strontium-89 (84).

Strontium-89 corresponded to nuclide B in the equations of Section V A and a half-life of 50.5 days (84) was used. The self-absorption corrections, f_β, for strontium-89, strontium-90, and yttrium-90 were 0.01, 0.05, and 0.00 respectively. The observed half-life of strontium-89 was 55.7 days. The data and results are given in Table 3. The yield of mass number 89 was

$$Y_{89} = \frac{9.2 \times 10^7}{K_2} \text{ disintegrations per second.}$$

3. Mass number 90

Strontium-90 was used to determine the fission yield of mass number 90. The strontium-90 activity was found by milking and counting its daughter, yttrium-90. The concentration of the yttrium carrier solution was not known precisely, but was taken to be one milligram of yttrium per milliliter; as this carrier solution was also used to prepare the yttrium standards in the spectrophotometric determinations, the yttrium counting factor could be found. The identity of the yttrium-90 was confirmed by observing its half-life. The low

Table 3. Experimental data and calculated results: mass number 89 -- thorium sample 2

Sr carrier (mg Sr)	98.5
Sr recovered (mg $SrC_2O_4 \cdot H_2O$)	9.2
Sr recovery (%)	4.23
Sr counting aliquot	0.01
$(Total)_c$ (c/m - background)	10,750
$(Sr\text{-}90 + Y\text{-}90)_c$ (c/m)	350
$(Sr\text{-}89)_c$ (c/m)	10,400
$(Sr\text{-}89)_c$ (d/m)	10,500
Sr counting factor	0.000423
$(\lambda_{Sr}N_{Sr})_c$ (d/s)	4.12×10^5
T_2 (days)	37.38
$(\lambda_{Sr}N_{Sr})_s$ (d/s) (Equation 6)	6.9×10^5
T_s (days)	49.58
T_o (days)	1.083
y_{89} (d/s) (Equation 3)	$\frac{9.2 \times 10^7}{K_2}$

counting rate of the Geiger-Müller yttrium samples prevented an estimation of the maximum beta-ray energy.

Strontium-90 and yttrium-90 corresponded to nuclides B and C respectively in the equations of Section V A and half-lives of 27.7 years and 64.2 hours respectively (84) were used. The self-absorption correction, f_β, for yttrium-90 was 0.00. The observed half-lives of two yttrium samples were

64 ± 7 and 61 ± 7 hours. The data and results are given in Table 4. The yield of mass number 90 was

$$Y_{90} = \frac{9.6 \times 10^7}{K_2} \text{ disintegrations per second.}$$

Table 4. Experimental data and calculated results: mass number 90 -- thorium sample 2

Sr carrier (mg Sr)	98.5			
Sr recovered (mg $SrC_2O_4 \cdot H_2O$)	9.2			
Sr milking aliquot	0.30		0.30	
Y carrier (mg Y)	1		1	
Y counted (mg Y)	0.136	0.136	0.131	0.131
$(Y\text{-}90)_c$ (c/m - background)	796	620	436	416
$(Y\text{-}90)_c$ (d/s)	13.3	10.3	7.3	6.9
Y counting factor	0.136	0.136	0.131	0.131
$(\lambda_Y N_Y)_c$ (d/s)	98	76	56	53
T_3 (hours)	5.33	8.45	38.7	44.25
T_m	43.34 days = 0.119 years			
$(Sr\text{-}90)_s$ (d/s) (Equation 7)	104	84	85	86
$(Sr\text{-}90)_s$ (d/s) (ave.)	94		86	
$(Sr\text{-}90)_s$ (d/s) (ave.)	90			
Sr recovery (%)	4.23			
$(\lambda_{Sr} N_{Sr})_s$ (d/s)	7.1×10^3			
T_s	49.52 days = 0.136 years			
T_o	1.083 days = 0.0029 years			
Y_{90} (d/s) (Equation 3)	$\frac{9.6 \times 10^7}{K_2}$			

4. Mass number 91

Yttrium-91 was used to determine the fission yield of mass number 91. The yttrium carrier solution was taken to be one milligram of yttrium per milliliter (see mass number 90). At the time of counting, the shorter-lived yttrium-90, initially present in the separated yttrium, had decayed to a negligible value. The identity of the yttrium-91 activity was confirmed by observing its half-life; the range of the activity in aluminum gave an estimate of the maximum beta-ray energy compatible with that of yttrium-91 (84).

The half-life of the yttrium-91 precursor, strontium-91, was not small compared with the time of the neutron irradiation. Strontium-91 and yttrium-91 corresponded to nuclides A and B respectively in the equations of Section V A, and half-lives of 9.67 hours and 57.5 days respectively (84) were used. The self-absorption correction, f_β, for yttrium-91 was 0.01.

The observed half-life of the yttrium activity was 60 days. The data and results are given in Table 5. The mass yield was found as

$$(1.007)y_{Sr} + y_Y = \frac{5.7 \times 10^7}{K_2} \ \frac{\text{disintegrations}}{\text{second}} .$$

For $y_{91} = y_{Sr} + y_Y$

and $y_{Sr} \gg y_Y$,

then $y_{91} = \frac{5.65 \times 10^7}{K_2}$ disintegrations per second.

Table 5. Experimental data and calculated results: mass number 91 -- thorium sample 2

Y carrier (mg Y)			1	
Y counted (μg Y)	3.24	3.24	3.24	3.24
$(Y\text{-}91)_c$ (c/m - background)	58,400	58,000	58,850	57,850
$(Y\text{-}91)_c$ (c/s)	973	967	981	964
$(Y\text{-}91)_c$ (d/s)	983	977	991	974
Y counting factor	3.24×10^{-3}	3.24×10^{-3}	3.24×10^{-3}	3.24×10^{-3}
$(\lambda_Y N_{Y\ c}$ (d/s)	3.03×10^{5}	3.01×10^{5}	3.06×10^{5}	3.01×10^{5}
T_2 (days)	43.31	44.04	44.19	44.26
$(\lambda_Y N_Y)_s$ (d/s) (Equation 6)	5.11×10^{5}	5.13×10^{5}	5.21×10^{5}	5.13×10^{5}
$(\lambda_Y N_Y)_s$ (d/s) (ave.)		5.14×10^{5}		
T_s (days)		30.17		
T_o (days)		1.083		
$K_2(1.007\ y_{Sr}+y_Y)$ (d/s) (Equation 2)		5.7×10^{7}		
y_{91} (d/s) (for $y_{Sr} \gg y_Y$)		$\frac{5.65 \times 10^{7}}{K_2}$		

5. Mass number 99

Molybdenum-99 was used to determine the fission yield of mass number 99. The identity of the molybdenum activity was confirmed by observing its half-life; the range of the

activity in aluminum gave an estimate of the maximum beta-ray energy compatible with that for molybdenum-99 (84).

The counting samples also contained the molybdenum-99 daughter, technetium-99m. Molybdenum-99 and technetium-99m corresponded to nuclides B and C respectively in the equations of Section V A, and half-lives of 66 and 6.0 hours respectively (84) were used. At the time of counting, the samples had a molybdenum-99 to technetium-99m activity ratio of 10:11 (Equation 7, Section V A). The counting efficiency for technetium-99m, a pure gamma-ray emitter, was taken to be one per cent. The self-absorption correction, f_β, for molybdenum-99 was 0.01.

The observed half-lives of two molybdenum samples were 66.3 and 65.3 hours. The data and results are given in Table 6. The fission yield of mass number 99 was

$$Y_{99} = \frac{2.2 \times 10^7}{K_1} \text{ disintegrations per second.}$$

6. Mass number 141

Cerium-141 was used to determine the fission yield of mass number 141. The cerium sample also contained cerium-144 and its daughter, praseodymium-144. To determine the ratio of the activity of cerium-141 to the activities of cerium-144 and praseodymium-144, a cerium sample was counted twice in the four-pi counter with about five weeks between the countings. By using published values for the half-lives and correcting

Table 6. Experimental data and calculated results: mass number 99 -- thorium sample 1

Mo carrier (mg Mo)	1.99	1.99
Mo counted (μg Mo)	4.14	7.44
$(Total)_c$ (c/m - background)	7660	13,370
$(Tc)_c$ (c/m)	84	147
$(Mo)_c$ (c/m)	7576	13,223
$(Mo)_c$ (d/m)	7650	13,350
$(Mo)_c$ (d/s)	128	222
Mo counting factor	0.00208	0.00374
$(\lambda_{Mo} N_{Mo})_c$ (d/s)	6.12×10^4	5.95×10^4
$T_2 + T_s$ (hours)	416.7	419.9
T_o (hours)	24	24
$K_1 y_{99}$ (d/s) (Equations 6 and 3)	2.17×10^7	2.18×10^7
y_{99} (d/s) (ave.)	$\frac{2.2 \times 10^7}{K_1}$	

for self-absorption, this activity ratio at the time of the second counting, and then at other times of interest, was found.

The identity of the cerium-141 was confirmed by observing its gamma-ray spectra (36). An estimate of its maximum beta energy was hampered by the presence of cerium-144 and praseodymium-144. The half-life data were compatible with a cerium-141 and cerium-144 mixture. These data could be

resolved into two components having half-lives of 33 and 295 days by calculating the cerium-141 to cerium-144 and praseodymium-144 activity ratios and by assuming that the relative beta-ray counting efficiencies for cerium-141, cerium-144, and praseodymium-144 were 0.3, 0.2, and 1.0 respectively. These efficiencies would be reasonable under the Geiger-Müller counting conditions.

Cerium-141 corresponded to nuclide B in the equations of Section V A. For cerium-141, cerium-144, and praseodymium-144, half-lives of 33.1 days, 285 days, and 17.3 minutes respectively (84) and self-absorption corrections, f_β's, of 0.05, 0.08, and 0.00 respectively were used. The data and results are given in Table 7. The yield of mass number 141 was

$$y_{141} = \frac{8.4 \times 10^7}{K_2} \text{ disintegrations per second.}$$

7. Mass number 143

Praseodymium-143 was used to determine the fission yield of mass number 143. The identity of the praseodymium-143 activity was confirmed by observing its half-life. The range of its beta-rays in aluminum gave an estimate of the maximum beta-ray energy compatible with that for praseodymium-143 (84). No gamma-rays were found using the 256 Channel Analyzer Spectrometer, which agrees with the published decay scheme of praseodymium-143 (84).

The half-life of the praseodymium-143 precursor, cerium-

Table 7. Experimental data and calculated results: mass number 141 -- thorium sample 2

Ce carrier (mg Ce)		1.00	
Ce counted (μg Ce)	3.16	0.804	0.804
$(\text{Total})_c$ (c/m - background)	160,200[a]	34,200	34,400
(Ce-141/Ce-144 + Pr-144)$_c$	2.00	1.89	1.89
(Ce-141) (d/m)	83,900	17,400	17,500
(Ce-141) (d/s)	1398	290	292
Ce counting factor	3.16×10^{-3}	0.804×10^{-3}	0.804×10^{-3}
$(\lambda_{Ce}N_{Ce})_c$ (d/s)	4.45×10^5	3.61×10^5	3.63×10^5
T_2 (days)	39.26	42.44	42.48
$(\lambda_{Ce}N_{Ce})_s$ (d/s) (Equation 6)	1.01×10^6	8.8×10^5	8.8×10^5
$(\lambda_{Ce}N_{Ce})_s$ (d/s) (ave.)		9.2×10^5	
T_s (days)		34.18	
T_o (days)		1.083	
y_{141} (d/s) (Equation 3)		$\frac{8.4 \times 10^7}{K_2}$	

[a]Corrected for a counting dead-time of 5 microseconds.

143, was not small compared with the time of the neutron irradiation. Cerium-143 and praseodymium-143 corresponded to nuclides A and B respectively in the equations of Section V A, and half-lives of 33 hours and 13.76 days respectively (84)

were used. The self-absorption correction, f_β, for praseodymium-143 was 0.02.

The observed half-life of the praseodymium-143 was 13.8 days. The data and results are given in Table 8. The mass yield was found as

$$(1.11\ y_{Ce} + y_{Pr}) = 9.3 \times 10^7 \frac{\text{disintegrations}}{\text{second}} .$$

For $y_{143} = y_{Ce} + y_{Pr}$

and $y_{Ce} \gg y_{Pr}$,

then $y_{141} = 8.4 \times 10^7$ disintegrations per second.

8. Mass number 144

Cerium-144 was used to determine the fission yield of mass number 144. The cerium sample also contained the cerium-144 daughter, praseodymium-144, and cerium-141. The ratio of the cerium-141 activity to the cerium-144 and praseodymium-144 activities was found as described under mass number 141.

The identity of the cerium-144 was confirmed by milking and counting the praseodymium-144 daughter. Estimates of the maximum beta-ray energies were compatible with a cerium-141 and cerium-144 mixture, and in good agreement with the strong beta-ray of praseodymium-144 (84). The half-life data of the cerium sample were compatible with a cerium-141 and cerium-144 mixture and could be resolved into two components having half-lives of 33 days and 295 days under reasonable assumptions

Table 8. Experimental data and calculated results: mass number 143 -- thorium sample 2

Pr carrier (mg Pr)	1.00	
Pr counted (mg Pr)	0.0049	0.0049
$(Pr\text{-}143)_c$ (c/m - background)	41,370	40,650
$(Pr\text{-}143)_c$ (d/m)	42,200	41,460
$(Pr\text{-}143)_c$ (d/s)	703	691
Pr counting factor	0.0049	0.0049
$(\lambda_{Pr}N_{Pr})_c$ (d/s)	1.43×10^5	1.41×10^5
T_2 (days)	36.28	36.33
$(\lambda_{Pr}N_{Pr})_s$ (d/s) (Equation 6)	8.9×10^5	8.8×10^5
$(\lambda_{Pr}N_{Pr})_s$ (d/s) (ave.)	8.8×10^5	
T_s (days)	34.18	
T_o (days)	1.083	
K_2 $(1.11\ y_{Ce} + y_{Pr})$ (d/s) (Equation 2)	9.3×10^7	
y_{143} (d/s) (for $y_{Ce} \gg y_{Pr}$)	$\frac{8.4 \times 10^7}{K_2}$	

(see mass number 141). The observed half-life of the milked praseodymium was 17.3 minutes.

Cerium-144 and praseodymium-144 corresponded to nuclides B and C respectively in the equations of Section V A, and half-lives of 285 days and 17.3 minutes respectively (84) were used. Because of the short half-life of praseodymium-144, the

praseodymium-144 activity was equal to the cerium-144 activity at the times of counting the cerium samples (Equation 7, Section V A). The self-absorption corrections, f_β's, for cerium-144 and praseodymium-144 were 0.08 and 0.00 respectively. The data and results are given in Table 9. The yield of mass number 144 was

$$y_{144} = \frac{9.2 \times 10^7}{K_2} \text{ disintegrations per second.}$$

9. Mass number 147

Neodymium-147 was used to determine the fission yield of mass number 147. The neodymium sample also contained the neodymium-147 daughter, promethium-147. The identity of the neodymium-147 was confirmed by observing its half-life; the half-life data could be resolved to give a half-life of 10.9 days by calculating the neodymium-147 to promethium-147 activity ratios (Equation 7, Section V A) and assuming that the relative beta-ray counting efficiencies were 1.0 and 0.5 for neodymium-147 and promethium-147 respectively. These efficiencies would be reasonable under the Geiger-Müller counting conditions. The range of the neodymium activity in aluminum gave an estimate of the maximum beta-ray energy compatible with that for neodymium-147 (84), and the gamma-ray spectrum agreed with that for neodymium-147 (84).

Neodymium-147 and promethium-147 corresponded to nuclides B and C respectively in the equations of Section V A, half-

Table 9. Experimental data and calculated results: mass number 144 -- thorium sample 2

Ce carrier (mg Ce)		1.00	
Ce counted (μg Ce)	3.16	0.804	0.804
$(\text{Total})_c$ (c/m - background)	160,200[a]	34,200	34,400
$(\text{Ce-141/Ce-144 + Pr-144})_c$	2.00	1.89	1.89
$(\text{Ce-144})_c$ (d/m)	41,900	9200	9250
$(\text{Ce-144})_c$ (d/s)	698	153	154
Ce counting factor	3.16×10^{-3}	0.804×10^{-3}	0.804×10^{-3}
$(\lambda_{Ce}N_{Ce})_c$ (d/s)	2.21×10^5	1.90×10^5	1.91×10^5
(T_2) (days)	39.26	42.44	42.48
$(\lambda_{Ce}N_{Ce})_s$ (d/s) (Equation 6)	2.43×10^5	2.11×10^5	2.12×10^5
$(\lambda_{Ce}N_{Ce})_s$ (d/s) (ave.)		2.22×10^5	
T_s (days)		34.18	
T_o (days)		1.083	
Y_{144} (d/s) (Equation 3)		$\frac{9.2 \times 10^7}{K_2}$	

[a]Corrected for a counting dead-time of 5 microseconds.

lives of 11.06 days and 2.64 years respectively (84) were used, and the self-absorption corrections, f_β's, were 0.04 and 0.10 respectively. The data and results are given in Table 10. The yield of mass number 147 was

$$y_{147} = \frac{3.4 \times 10^7}{K_2} \text{ disintegrations per second.}$$

Table 10. Experimental data and calculated results: mass number 147 -- thorium sample 2

Nd carrier (mg Nd)	1.00	
Nd counted (mg Nd)	0.0304	0.0304
$(\text{Total})_c$ (c/m - background)	36,980	38,400
$(\text{Pm-147/Nd-147})_c$ (Equation 7)	0.149	0.149
$(\text{Nd-147})_c$ (d/m)	33,800	35,000
$(\text{Nd-147})_c$ (d/s)	563	583
Nd counting factor	0.0304	0.0304
$(\lambda_{Nd}N_{Nd})_c$ (d/s)	1.85×10^4	1.92×10^4
T_2 (days)	42.35	42.40
$(\lambda_{Nd}N_{Nd})_s$ (d/s) (Equation 6)	2.62×10^5	2.73×10^5
$(\lambda_{Nd}N_{Nd})_s$ (d/s) (ave.)	2.67×10^5	
T_s (days)	34.18	
T_o (days)	1.083	
y_{147} (d/s) (Equation 3)	$\frac{3.4 \times 10^7}{K_2}$	

B. Summary of Calculated Results

The mass yields determined in this work are given in Table 11. The yields relative to mass number 140 and the absolute yields based on y_{140} = 6.2 per cent (45) are also given. The relative yields are plotted as a fission-yield

Table 11. Mass yields in the pile-neutron irradiation of thorium-232

Mass number	Yield: R/K x 10^{-7} (disintegrations/second)	Relative yield	Absolute yield (%)
140	$\frac{5.45 \pm 0.2}{K_1}$	1.00	6.2 (45)
140	$\frac{8.8 \pm 0.45}{K_2}$	1.00	6.2
89	$\frac{9.2 \pm 0.4}{K_2}$	1.04 ± 0.06	6.4 ± 0.4
90	$\frac{9.6 \pm 0.4}{K_2}$	1.09 ± 0.06	6.8 ± 0.4
91	$\frac{5.65 \pm 0.2}{K_2}$	0.64 ± 0.04	4.0 ± 0.25
99	$\frac{2.2 \pm 0.1}{K_1}$	0.40 ± 0.03	2.5 ± 0.2
141	$\frac{8.4 \pm 0.3}{K_2}$	0.95 ± 0.06	5.9 ± 0.4
143	$\frac{8.4 \pm 0.3}{K_2}$	0.95 ± 0.06	5.9 ± 0.4
144	$\frac{9.2 \pm 0.4}{K_2}$	1.04 ± 0.06	6.4 ± 0.4
147	$\frac{3.4 \pm 0.1}{K_2}$	0.39 ± 0.03	2.4 ± 0.2

curve in Figure 1 together with mirror yields reflected about mass number 115.

The errors arose mainly from three sources: (1) errors in the per cent recovery and the counting factor, (2) error in converting the observed counting rate to the disintegration rate, and (3) calculation error.

1. Errors in the per cent recovery and the counting factor

For mass numbers 140, 89 and 90, the per cent recovery depended on weighing barium chloride or strontium oxalate precipitates. Deviations from exact stoichiometric compounds were neglected because the carrier solutions for these elements were standardized by weighing the same precipitates under similar conditions. The errors were taken to be one per cent for strontium and barium (thorium sample 1) and two per cent for barium (thorium sample 2).

For other mass numbers the counting factors depended on volumetric procedures and spectrophotometric analyses. The error was taken to be one per cent.

2. Error in converting the observed counting rate to the disintegration rate

In all cases the counting statistics were such as to give a standard deviation of less than one per cent in the observed counting rate. The loss of beta radiation due to absorption in the sample film was neglected. This loss could be as high as one per cent for the weakest beta-ray emitter, promethium-147, but was less for the others.

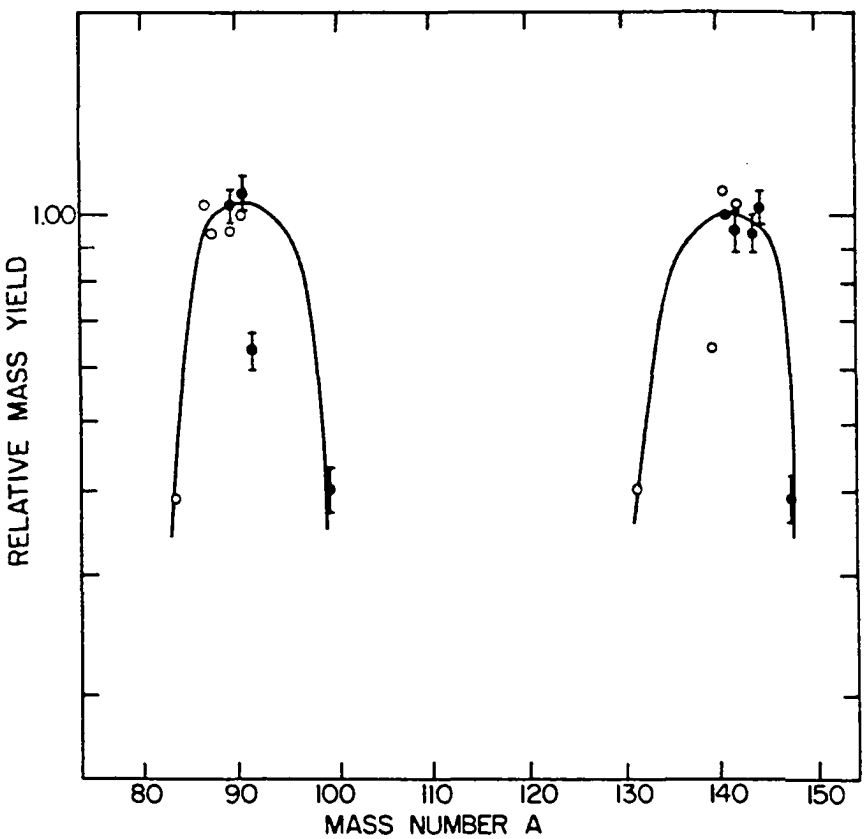

Figure 1. Relative fission-yield curve of thorium-232 for pile neutrons; •, yields for nuclide of mass A; ∘, mirror points for 230-A; solid curve from reference 45

The loss of beta radiation due to self-absorption was estimated from the expression,

$$\log(1 - f_\beta) = -0.80 - E_\beta(\text{Mev.})\,(31),$$

where E_β = the maximum beta-ray energy,

and $$1 - f_\beta = \frac{\text{net counting rate}}{\text{disintegration rate}} .$$

The f_β values are given in Table 12 and are similar to other measured values for self-absorption (63).

Table 12. The self-absorption corrections

Nuclide	f_β	Nuclide	f_β
La-140	0.01	Ce-141	0.05
Sr-89	0.01	Pr-143	0.02
Sr-90	0.05	Ce-144	0.08
Y-90	0.00	Pr-144	0.00
Y-91	0.01	Nd-147	0.04
Mo-99	0.01	Pm-147	0.10

These corrections are only approximate but appear to be valid for counting samples of about 30 micrograms per square centimeter or less. Reducing the samples below an apparent density of 30 micrograms per square centimeter does not lower the self-absorption correction, presumably because the sample materials form aggregates of about this density rather than remain spread out to give lower densities (74). Any additional self-absorption loss in the strong beta-ray emitters,

lanthanum-140 (thorium sample 1) and yttrium-90, having sample densities of about 160 and 130 micrograms per square centimeter respectively, are neglected. The error due to uncertainties in converting the observed counting rate to a disintegration rate was taken to be two per cent.

3. Calculation error

The principal sources of error in the calculations of Section V A are due to the assumption that the fissioning-neutron flux was constant during the irradiation and to uncertainties in the decay constants. The effect of the latter can be seen from Equations 2 or 3; the yield is proportional to $\frac{1}{(1 - e^{-\lambda T_o})}$. For the present work $(1 - e^{-\lambda T_o})$ is about equal to (λT_o), so that the error in the calculated yield is about equal to the error in λ. The decay constants used were the best available (84) and these errors were neglected.

The effect of a non-constant neutron flux upon the calculated yields, to a rough approximation, is about equal to $\frac{1}{K\lambda T_o}$, using $(1 - e^{-\lambda T_o}) \tilde{=} \lambda T_o$; in this case any change in the flux would affect all yields equally and leave the relative yields unchanged. For the nuclides studied, this approximation is least valid for molybdenum-99, which would be the most sensitive to a changing flux. This error was neglected.

IV. DISCUSSION

A. Comparison with Other Work

The mass number yields produced in the pile-neutron fission of thorium-232 obtained by this work are shown in Figure 1. These yields are relative to the yield of mass number 140. The data indicate the light and heavy peaks of asymmetric fission; this is emphasized by plotting the mirror yields, reflecting about mass number 115. The yields for mass numbers 143 and 147 appear to be in agreement with the other yields. The only serious discrepancy may be the yield of mass number 91 which appears to be about 35 per cent low. Yield data in the trough region were not obtained. The accuracy of the data does not permit the determination of any fine structure in the yield curve.

The average energy of the fission-inducing neutrons was calculated by using the neutron-energy distribution in the CP-5 reactor, that is, the fission-neutron spectrum for the thermal neutron fission of uranium-235 (77, p. 621), and the fission cross section as a function of neutron energy (39). The neutron energy spectrum is given as N(E) which is the number of neutrons with energy E to E + dE per fission neutron. The neutron flux, nv, is proportional to N(E) since n, the density of neutrons with energy E to E + dE, is proportional to $\frac{N(E)}{v}$, where v is the velocity of the neutrons.

The neutron flux (or N(E)), the fission cross section, σ_f, and the fission reaction probability, (nv) x σ_f, are plotted against neutron energy in Figure 2. The average energy of the neutrons causing fission was estimated to be 3.3-Mev; less than 10 per cent of the fissions were caused by neutrons having energies greater than 6-Mev.

The mass yields in the pile-neutron irradiation of thorium-232 have been determined by Turkevich and Niday (96). They estimated that half of the fissions were caused by neutrons having energies greater than 2.7-Mev. Their yields were measured relative to mass number 89 and about half of their data depended upon mass yields in the thermal-neutron fission of uranium-235. Their data were corrected by using more recent uranium-235 thermal fission yields (45) and calculated relative to mass number 140. A smooth curve of their data is given in Figure 1; their trough data are omitted. Within their estimated error of $\pm$ 20 per cent ($\pm$ 50 per cent for mass number 141), the yields obtained in this work agree except for the yield of mass number 91.

B. Asymmetric and Symmetric Fission

Since the discovery of fission, various models have been used or proposed to explain the fission process ranging from the first, simple liquid-drop model (6) to involved statistical models (20). One of the interesting aspects of fission has

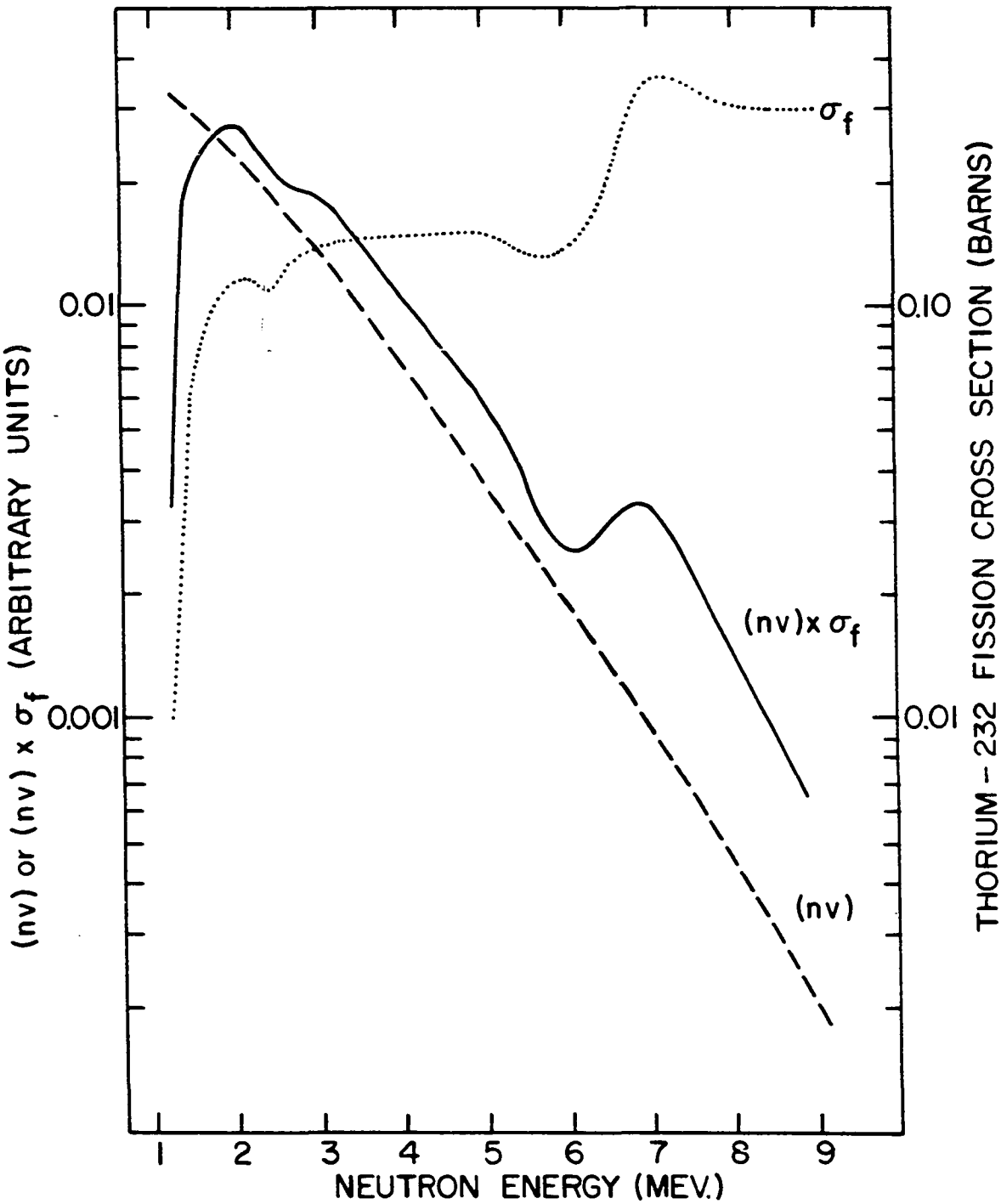

Figure 2. Variation with neutron energy of a, neutron flux (nv); b, thorium-232 fission cross section, σ_f; c, (nv) x σ_f

been that all of the models have predicted that symmetrical fission should be the predominant fission mode, while experimental observations have shown that asymmetrical fission predominates (34).

Since the mass-yield curve of the thermal-neutron fission of uranium-235 was determined, the mass-yield curves of various target nuclei have been determined using increasingly energetic bombarding particles. The yields in the neutron fission of thorium-232 with neutrons of greater-than-pile energies have been determined by Turkevich et al. (97) and by Alexander and Coryell (1).

Turkevich et al. (97) bombarded lithium with 7.6-Mev. deuterons to obtain neutrons with a maximum energy of 21-Mev. Their calculations indicated that most of the neutrons had energies less than 14-Mev., that about 10 per cent of the fission events were induced by neutrons with energies greater than 14-Mev., and that a majority of fission events were caused by neutrons with energies between 6- and 11-Mev. Their error was generally about 20 per cent and could not indicate any fine structure in the yield curve. The ratio of the valley or trough of the yield curve to the peak of the yield curve was about 0.1. The valley-to-peak ratio obtained in the pile-neutron fission of thorium(96) was about 0.01. Using the valley-to-peak ratio as a measure of the symmetrical-to-asymmetrical fission ratio, they decided that this ratio

increases with increasing fissioning energy. Alexander and Coryell (1) used 0- to 19-Mev neutrons from the beryllium-deuteron reaction to bombard thorium with similar results.

These data, along with the pile-neutron fission yields (96), are shown as smooth curves in Figure 3. The mass yields were relative to the yield of mass number 89. The increase in the valley-to-peak ratio is clearly shown.

Another study (76) of thorium-232 fission, using 14.9-Mev. neutrons, gave the most probable mass ratio as 1.43 $\pm$ 0.03, and the masses of the heavy and light fission fragments as 140 $\pm$ 3 and 92 $\pm$ 3 respectively. This would give an estimate of the valley-to-peak ratio of about 1/6. A study (44) of the distribution of kinetic energy of fission fragments with the mass number of the fragments in the fission of thorium-232 with high-energy neutrons showed two peaks with about a twenty per cent dip between them at 45-Mev. and a single peak at 90-Mev.

A compilation (85) of valley-to-peak ratios in the fission of various target nuclei by various particles of various energies to give excitation energies from 5- to 30-Mev. showed the general increase of the valley-to-peak ratio with increasing excitation energy.

From this, it appeared that the lower the excitation energy the more the asymmetric fission mode predominates. The lowest excitation energy would be for spontaneous fission.

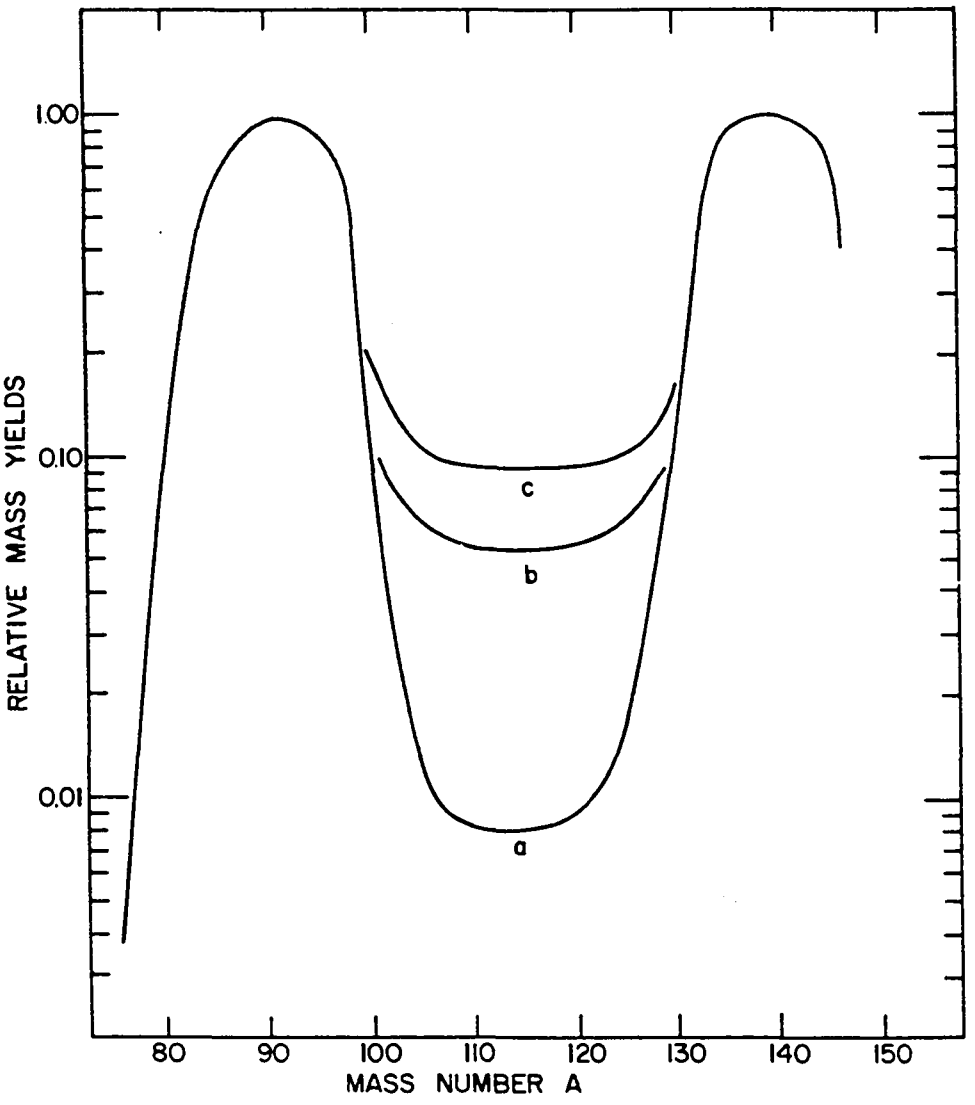

Figure 3. Fission-yield curves for thorium-232; a, pile-neutrons (96); b, 0- to 19-Mev. neutrons (1); c, 0- to 21-Mev. neutrons (97)

A mass spectrometric study (102) of xenon and krypton isotopes in old uranium and thorium ores gave an indication of very sharp fission-yield curve peaks, characteristic of asymmetric fission, in what was considered to be spontaneous fission of uranium and thorium.

The general increase in the relative amount of symmetric fission with an increase in excitation energy does not appear to occur at lowest excitation energies. A radiochemical investigation (66) has indicated no difference in the ratio of the yields of mass number 115 and 89, corresponding to the valley-to-peak ratio, in the fission of uranium-235 with resonance neutrons of 1.1-, 3.1-, and 9.0-Ev. A second study (11) measuring the silver-111-to-molybdenum-99 ratio, mainly in the 10- to 60-Ev. region, has indicated no appreciable symmetric fission in the first five hundred resonances up to 1000-Ev. of uranium-235. A third study (4) has shown perhaps even greater asymmetry for fission of uranium-235 by resonance neutrons over fission by thermal neutrons.

A possible explanation of the lack of symmetric fission at low excitation energies is given by Newson (64) who considers $_{50}Sn^{132}_{82}$, a doubly magic nuclide, as the core for the heavy mass peak. To disrupt this core would cost several Mev. This may also help explain the fact that in the fission of various nuclides, the heavy peak remains relatively constant while the light peak changes as the mass of the fissioning

nuclide changes.

The mass distributions of both the symmetric and asymmetric fission modes for the neutron fission of uranium-235 apparently do not change with energy in fission from 2- to 10-Mev. (mean neutron energies) although the relative proportion of the modes change. However, comparison of these results with thermal-neutron fission data of uranium-235 indicated disagreement with the assumption of constant mass distribution with energy for the fission modes (54).

A general review of asymmetric fission is given by Halpern (34).

The extent of ternary fission of thorium by neutrons has been found to be small. In the fission of uranium-235 by neutrons, the presence of a third fission fragment has been observed with photographic plates (93). This third fragment occurred about once in a hundred fissions and was either a short-range or a long-range fragment. The proportion of long-range fragments was greatest in thermal-neutron fission and decreased with increasing neutron energy. Ternary fission of thorium with fast neutrons has also been observed to occur once in a hundred fissions (16) but only short-range fragments were found (16, 94). However, another photographic study found only twelve ternary fission tracks in 14,000 binary fissions of thorium by 2.5-Mev. neutrons (90) and five ternary tracks in 2500 binary photofissions of thorium(92). The

ternary fragments are generally considered to be alpha particles (90, 93) although two beryllium-8 nuclei were observed in 640,000 fissions of uranium-235, uranium-238, and thorium-232 (91).

No quatenary fission has been observed in the fission of thorium-232 or uranium-238 but two cases have been reported in about 10,000 cases of neutron fission of uranium-235 (95).

C. Reactions at Higher Excitation Energies

An increase in excitation energy increases the number of possible reactions. Thorium-232 has a half-life for spontaneous fission estimated to be 10^{21} years or longer (19) and a thermal-neutron fission cross section of 0.02 to 0.06 millibarns or less (26, 51). The capture of a neutron provides about 5-Mev. of excitation energy and the (n, f) reaction begins in earnest at a threshold neutron energy of 1.17-Mev. (39) or at an excitation energy of about 6-Mev. From the photofission threshold of 5.4-Mev. (49), assuming that emitted neutrons of 1-Mev. energy would decrease the excitation energy by about 7-Mev., the (n, nf) reaction begins with bombarding neutrons of 6- to 7-Mev. At higher neutron energies (n, 2nf), (n, 3nf), etc. begin.

The investigation of high-energy fission requires in the case of fission by neutrons the production of these neutrons through bombardment of targets such as deuterium, lithium, or

beryllium with accelerated charged particles, hence the neutron fluxes are low. For this reason, the bulk of high-energy fission work has been charged-particle fission.

The presence of (p, xnf) reactions and the increase in the symmetric-to-asymmetric fission ratio with increasing excitation energy has been shown in the proton fission of thorium-232 (7). The symmetric-to-asymmetric fission ratio, measured by the relative yields of mass numbers 113 and 139, increased with increasing proton energy with discontinuities at proton energies of 8.0-, 14.0-, 23.6-, 29.5-, 40-, and 48-Mev. With 8-Mev. protons, the emission of a neutron produced a nucleus of lower-excitation energy which would have a lower symmetric-to-asymmetric fission ratio.

With higher energy charged particles, apparently two stages occur. The first stage, nucleonic cascade, is a direct interaction between the projectile and nucleons of the target nucleus producing charged particles and spallation products (80). Since the emission of protons by evaporation from an excited nucleus is very low at excitation energies below 100-Mev. (41), reactions such as (alpha, p2n), (d, p2n), and (p, p2n) at moderate energies of 48-, 24-, and 32-Mev. respectively can thus be explained (99). This first stage is followed by compound nucleus formation in which evaporation of neutrons and fission compete (22, 30). Work on reactions with thorium by protons with energies of up to 100-Mev. (7)

and 340-Mev. (56), and of 0.68- and 1.8-Bev. (71) agree with the two-stage process. The reactions of thorium plus 380-Mev. alphas, 190-Mev. deuterons, and 340-Mev. protons produced fission products which were neutron-deficient, which may indicate that the fission process was preceded by the loss of up to twenty-five nucleons, mainly neutrons, through the cascade or evaporation stages (55).

Spallation and fission products of many alpha, deuteron, and proton reactions with thorium are given by Thomas et al. (89). High-energy reactions were reviewed by others (35, 65).

D. Fine Structure in Fission

The yield curve for the thermal-neutron fission of uranium-235 was originally drawn as a smooth curve with the two peaks of asymmetric fission (10, p. 2009). However, mass spectrometric studies of krypton and xenon fission isotopes showed the presence of fine structure in the yield curve, with krypton-85 and xenon-134 yields about 35 per cent too high to fit on the smooth curve (88). Also the xenon-136 yield was about 6.1 per cent (88) while the iodine-136 yield was only about 3.1 per cent (81); as this could not be explained by neutron capture by xenon-135 or delayed-neutron emission by xenon-137 (46), it seemed to require an independent yield of xenon-136 far higher than expected.

To explain this, Glendenin (28) postulated that after

emitting prompt neutrons, primary fission fragments, which contained one neutron in excess of a closed shell (i.e., 51 or 83 neutrons), lose this neutron rather than emit a beta- or gamma-ray, causing cross-chain branching. Using this chain branching mechanism and estimating independent yields in mass chains for the 82 neutron region, the high yields of xenon-134 and xenon-133, and the low yield of iodine-136 were qualitatively explained (57).

With this postulate, the gain in the 133-134 mass yields should mean a loss in the 135-137 mass yields, but a study of cesium fission isotopes showed this not to be the case (103). Hence it was proposed that, in addition to the Glendenin chain branching mechanism, primary fission fragments with an 82-neutron closed shell had enhanced yields; this gave predicted yields in good agreement with observed yields from mass 132 to mass 137 in the thermal-neutron fission of uranium-235 (103). Pappas (68) extended the chain branching mechanism to include the third, fifth, and seventh neutrons in excess of the 82-neutron closed shell and obtained good agreement in the mass region from 130 to 150 except at masses 134 and 135, where predicted values were low and perhaps enhanced yields for 82-neutron fragments were required.

The Glendenin-Pappas mechanism predicts fine structure at masses 131-132 in the neutron fission of uranium-238 which has been found, but the predicted values are higher than

observed (101). This mechanism also predicts fine structure at masses 134-135 in the thermal-neutron fission of uranium-233, but the predicted values are much higher than observed and the fine structure, if present, is very small (18). The disappearance of fine structure in going from uranium-235 to uranium-233 is unexpected and as yet unexplained.

The closed-shell preference of fission fragments would give enhanced yields of fragments complementary to the 82-neutron fragments. A fine structure peak was found at mass 100 in the thermal-neutron fission of uranium-235 which seems best explained by the preference in fission for its 82-neutron complementary fragments (29).

A preference in fission for a 50-neutron shell would show up in the 84-85 mass region. Krypton yields in this region in the thermal-neutron fission of uranium-235 show fine structure (75, 101), but the yields predicted by the Glendenin-Pappas mechanism for fission fragments of 51, 53, 55, and 57 neutrons do not agree with the experimental yields (101). Since the light mass peak in asymmetric fission shifts to lower masses with lower mass of the fissioning nucleus, the fine structure in the 84-85 mass region should be more readily apparent in these cases as the yields are higher and do not change so rapidly with mass. The krypton yields in the thermal-neutron fission of uranium-233 indicated fine structure at mass numbers 84 and 85 (18).

The yields in the 84-85 mass region increase in going from uranium-238 to uranium-235 to uranium-233, indicating the shift of the light mass peak, but the fine structure decreases (18). A reasonably quantitative explanation of the fine structure in this mass region has been obtained for uranium-238, 235, and 233 neutron fission by assigning the 0.43 second delayed-neutron activity to arsenic-85, as the predicted relative yield of arsenic-85 in the 85 mass chain also decreases with decreasing uranium mass (17, 18). This would indicate that the 50-neutron shell preference in fission has little effect.

Fine structure has recently been observed in the fast-neutron fission of thorium-232 (47). Thorium, wrapped in cadmium, was placed in an uranium cylinder which in turn was placed in a lattice position that had an unperturbed thermal flux of about 8.2×10^{13} neutrons/sec.-cm.^{2} The fast-neutron flux inside the uranium cylinder was about 21 per cent of the unperturbed flux, and the cadmium reduced the thermal flux to about 2×10^{12} neutrons/sec.-cm.^{2} Three-week and six-week irradiations were run. Mass spectrometric methods were used to determine the relative yields of the krypton and xenon fission products. Isotopic dilution techniques, using a krypton-80, 82 and xenon-128 mixture, gave the krypton yields relative to the xenon yields. The absolute yields were obtained by fitting these on the yield curve of Turkevich and Niday (96) and

summing to 200 per cent total yield.

The absolute yields, given in per cent, were

krypton-83	1.99 ± 0.01	xenon-131	1.62 ± 0.01
krypton-84	3.65 ± 0.02	xenon-132	2.87 ± 0.02
krypton-85	3.88 ± 0.02	xenon-134	5.38 ± 0.03
krypton-86	6.00 ± 0.03	xenon-136	5.65 ± 0.03

The krypton-84 yield was high, the krypton-85 yield low; this could be due to cross-chain branching from the 85 mass chain to the 84 mass chain, perhaps by selenium-85, or possibly a fission structural preference is present. The xenon-131, 132, 134, and 136 yields give a slight indication of a combination of structural preference in fission and neutron emission by the Glendenin-Pappas mechanism. Comparison of the krypton yields with the yields of uranium fission shows that the thorium-232 fission fine structure most closely resembles the fine structure in uranium-238 fission, although the thorium yields are higher because of the shift of the light mass peak.

The effect of higher excitation energies on fine structure was shown by Wahl (100) in the fission of uranium-235 by 14-Mev. neutrons. The pronounced fine structure of thermal fission at mass number 134 is almost completely gone in 14-Mev. neutron fission. Perhaps those nuclei undergoing asymmetric fission have lost neutrons by evaporation and so would be better compared with thermal-neutron fission of uranium-233 (uranium-234 fissioning nucleus) than with thermal-neutron fission of uranium-235 (uranium-236 fissioning nucleus).

E. Charge Distribution in Fission

One of the interesting aspects of fission is the charge distribution, the division of the charge of the fissioning nucleus into the fission fragments. The obvious way to determine this distribution in a given mass chain is to determine the independent yields of the members of the chain; however most of the chain members have very short half-lives so that the experimental determination of the independent yields in a given mass chain is difficult. Hence, the independent yields of fission products of many mass chains, especially yields of shielded isotopes, have been determined and correlated to give the charge distribution in fission.

To correlate the data, two primary assumptions have been made: (1) that the charge distribution of a given mass was a Gaussian, symmetrical about a probable charge, and (2) that the distribution was the same for all masses. No theoretical treatment has agreed with the experimental data, but Glendenin's semi-empirical Equal-Charge-Displacement (ECD) postulate has (10, p. 489). The ECD postulated that the most probable charge of a light mass was equally displaced from the most stable charge of the light mass as the most probable charge of the heavy (complementary) mass was displaced from the most stable charge of the heavy mass. That is,

$$Z_A - Z_P = Z_{A*} - Z_{P*}$$

where Z_A and Z_{A*} are the most stable charges for complementary

mass numbers A and A*, and Z_p and Z_{p*} are the most probable charges of the primary fission products of mass numbers A and A*. Also,

$$Z_p + Z_{p*} = Z_F$$

and

$$A + A^* = A_F - \bar{\nu}$$

where Z_F and A_F are the charge and mass of the fissioning nucleus (target A + 1) and $\bar{\nu}$ is the average number of neutrons emitted per fission. The Z_A values were taken from the Bohr-Wheeler stability curve (6). The ECD means that the chain lengths are the same for all masses; the agreement of ECD results with the early data on thermal-neutron fission of uranium-235 was good (10, p. 489).

The Glendenin ECD postulate was improved with a modification by Pappas (68) that took into account the effect of n and p shells on stability. The Z_A values were taken from Coryell (9). Pappas also calculated the charge distribution of primary fragments rather than of final fission products since the prompt fission neutrons are emitted from the fragments (104), i.e.,

$$A + A^* = A_F.$$

The Glendenin-Pappas ECD results agree well with the thermal-neutron fission data of uranium-235; comparison of the Glendenin-Pappas ECD results with the Glendenin ECD results and with results of several other charge distribution treat-

ments is given for the thermal-neutron fission of uranium-235 by Pappas (68). The Glendenin-Pappas ECD results also agree with data from the slow-neutron fission of uranium-233, uranium-235, and plutonium-239, the fast-neutron fission of uranium-238 and thorium-232, and the spontaneous fission of curium-242 (82).

The ECD postulate requires a rearrangement of the proton density; since the low-energy fission process is slow (ca. 10^{-14} sec.), there is ample time for this rearrangement (68). Under the assumption that the fission process is faster at higher energies, it was felt that ECD mechanism would give place to a mechanism which would not require rearrangement, such as an unchanged charge distribution (UCD) (30). The charge distribution in the 14-Mev. neutron fission of uranium-235 indicates agreement with the ECD postulate with the most probable charge shifted toward stability (21, 100). This shift toward stability could be explained by an increase in the emission of neutrons before fission or perhaps after fission from the fragments (100). From a study of the fission of thorium and uranium with 13.6-Mev. deuterons plus consideration of the 14-Mev. fission of uranium-235 (21, 100) it was concluded that the ECD postulate can be extended to the fission of compound nuclei with atomic numbers 90 to 93 and excitation energies of 10 to 20 Mev. (1).

The yields of iodine and tellurium isotopes in the mass

range 130-135 were studied in the fission of thorium with 8- to 90-Mev. protons (70). The charge distribution curves at 8-, 24-, 45-, 64-, and 87-Mev. proton energy were plotted as fractional yield versus (Z_A - Z); the charge distributions from thermal- and 14-Mev. neutron fission of uranium-235 and the 170- and 480-Mev. proton fission of uranium were also plotted. The results indicated that with increasing energy of the bombarding particle, the charge distribution moved toward stability, rapidly at first, more slowly at higher energies, and that the width of the distribution was constant to about 25-Mev. but at higher energies increased with increasing energy. The shift in the charge distribution corresponded to a decrease in the n/p ratio of the fission products, and was interpreted as reflecting a decrease in the n/p ratio of the fissioning nucleus caused by nucleon evaporation (mainly neutrons) prior to fission with perhaps some contribution by neutron evaporation after fission from the fragments. The increased width was due to a wider range of fissioning nuclei, hence a wider distribution of n/p values in the fission products. A two-step model was proposed: (1) below 50-Mev. a compound nucleus was formed followed by de-excitation, and (2) above 50-Mev. direct nucleon interaction occurred followed by compound nucleus followed by de-excitation. The de-excitation was by nucleon evaporation with which fission competed.

In a more sophisticated study, the n/p ratios in the mass

range 130 to 135 in 8.0- and 87-Mev. proton fission of thorium and the n/p ratios of mass numbers 90 and 130 in the 450-Mev. proton fission of uranium were calculated (69). These ratios were compared with experimental values [thorium data (70), uranium data (53)]. The results indicate that fission of nuclides of atomic numbers 87 to 93 with excitation energies up to a few hundred Mev. proceeds predominantly via an ECD mechanism, not by UCD, and that fission competes in these nuclides with nucleon emission when Z^2/A values are greater than 36 in a fashion independent of energy. The results also indicate that the ECD mechanism occurs in the 480-Mev. proton fission of uranium.

The Glendenin-Pappas ECD mechanism was used to calculate estimated independent yields for the mass numbers investigated in this study. In the case of mass number 140, the estimated fractional yield of lanthanum-140 was about 0.001. This means that the yield of barium-140 (plus the yields of its short-lived precursors) would be about 99.9 percent of the yield for mass number 140. The effects of independent yields were estimated to be even less for the other mass numbers studied.

V. APPENDICES

A. Calculations

The mass yields were found by knowing the relationship between the activity of a particular isotope in a mass chain and the fission yield of that mass chain. This relationship was found by assuming:

(1) the fissioning-neutron flux was constant during the irradiation,

(2) the mass yields were either constant over the fast neutron spectra or any change in the mass yields were the same for all mass chains investigated, and

(3) in a particular mass chain, nuclide A was formed through fission and nuclide B was formed both through independent fission and through beta decay of nuclide A. That is, for nuclide A, the reaction was thorium (n, f)A, and for nuclide B, the reactions were thorium (n, f)B and A(beta decay)B.

1. The activity and yield of nuclide A

During the irradiation, the change with time of nuclide A was

$$\frac{dN_A}{dt} = (nv)\sigma_f N_{Th} y_A - \lambda_A N_A,$$

where N_A = the number of atoms of nuclide A,

(nv) = the fissioning-neutron flux,

σ_f = the fission cross section of thorium-232,

N_{Th} = the number of atoms of thorium-232,

y_A = the independent fission yield of nuclide A, and

λ_A = the decay constant of nuclide A.

Using $K = (nv)\sigma_f N_{Th}$, this becomes

$$\frac{dN_A}{dt} = Ky_A - \lambda_A N_A.$$

The activity of nuclide A at the end of the irradiation was

$$(\lambda_A N_A)_o = Ky_A(1 - e^{-\lambda_A T_o}),$$

where T_o = the duration of the irradiation.

After the irradiation, nuclide A decayed exponentially to give

$$(\lambda_A N_A)_c = (\lambda_A N_A)_o \, e^{-\lambda_A T_1},$$

where T_1 = the time between the end of the irradiation and the counting of nuclide A.

The yield of nuclide A could be calculated from $(\lambda_A N_A)_c$ by

$$y_A = \frac{(\lambda_A N_A)_c}{K(1 - e^{-\lambda_A T_o})(e^{-\lambda_A T_1})}.$$

This could be rewritten as

$$y_A = \frac{R_A}{K},$$

where $R_A = \dfrac{(\lambda_A N_A)_o}{1 - e^{-\lambda_A T_o}}$ = the saturation disintegration rate of nuclide A.

2. The activity and yield of nuclide B

The activity of nuclide B was formed both through independent fission and through the beta decay of nuclide A during

and after the irradiation. It can be shown that the total activity of nuclide B at the time of the separation of nuclide B from nuclide A was

$$(\lambda_B N_B)_s = K[y_B + y_A \frac{\lambda_A}{(\lambda_A-\lambda_B)}][1 - e^{-\lambda_B T_o}] e^{-\lambda_B T_s}$$

$$-Ky_A \frac{\lambda_B}{(\lambda_A-\lambda_B)} [1 - e^{-\lambda_A T_o}] e^{-\lambda_A T_s}, \quad (1)$$

where T_s = the time between the end of the irradiation and the separation of nuclide B.

Since in this work $\lambda_A \gg \frac{1}{T_s}$, Equation 1 simplified to

$$(\lambda_B N_B)_s = K[y_B+y_A \frac{\lambda_A}{(\lambda_A-\lambda_B)}][1 - e^{-\lambda_B T_o}]e^{-\lambda_B T_s} \quad (2)$$

for $\lambda_A > \lambda_B$, and to

$$(\lambda_B N_B)_s = K[y_B+y_A][1 - e^{-\lambda_B T_o}]e^{-\lambda_B T_s} \quad (3)$$

for $\lambda_A \gg \lambda_B$. These could be rewritten as

$$y_B + y_A \frac{\lambda_A}{(\lambda_A-\lambda_B)} = \frac{R_B}{K} \text{ for } \lambda_A > \lambda_B, \quad (4)$$

and

$$y_A+y_B = \frac{R_B}{K} \text{ for } \lambda_A \gg \lambda_B, \quad (5)$$

where

$$R_B = \frac{(\lambda_B N_B)_s}{(1 - e^{-\lambda_B T_o})(e^{-\lambda_B T_s})}.$$

After the separation, nuclide B decayed exponentially so that the activity of nuclide B at the time of counting was

$$(\lambda_B N_B)_c = (\lambda_B N_B)_s e^{-\lambda_B T_2}, \quad (6)$$

where T_2 = the time between the separation and counting of nuclide B.

The yield of nuclide B was calculated from $(\lambda_B N_B)_c$ by using Equation 6 and either Equation 2 or Equation 3.

The activity of nuclide B could be determined by milking and counting its daughter, nuclide C. It can be shown that the activity of nuclide C at the time of counting was

$$(\lambda_C N_C)_c = (\lambda_B N_B)_s \left(\frac{\lambda_C}{\lambda_B - \lambda_C}\right)(e^{-\lambda_C T_m} - e^{-\lambda_B T_m}) e^{-\lambda_C T_3} \qquad (7)$$

where T_m = the time between the separation of nuclide B and the milking of nuclide C, and

T_3 = the time between the milking and counting of nuclide C.

B. Four-Pi Sample Films

The four-pi sample films were prepared by dropping a tygon:tygon thinner (1:1) mixture onto a water surface. After evaporation of the thinner, the film was picked up on a wire frame and placed over an aluminum holder. This holder was a disk, 8.5 centimeters in diameter and 0.5 millimeters in thickness, which had a center aperture 2.5 centimeters in diameter. The thickness of the holder and the size of the aperture were such as to reduce the loss of beta-radiation due to absorption in the holder to a negligible amount (64, 72).

The films were coated with aluminum in a vacuum

evaporator at a pressure of about 0.2 microns (38, p. 255). About three inches of number 20 aluminum wire were used on a 30 mil tungsten helical filament. Eight films were coated at a time and the filament could usually be used twice. The films were coated until a good mirror was obtained but before the aluminum coat became opaque.

The density of the coated and uncoated films were found by using aluminum holders with a 6.8 centimeter aperture. Ten films were removed from these holders and weighed. The density of the coated and uncoated films were about 20 and 15 micrograms per square centimeter respectively. The density of the coated film was insufficient to produce an appreciable loss of beta-radiation by absorption (73). The density of the aluminum coat was large enough to make the film conducting (38, p. 207). The need for a conducting film in four-pi counting has been questioned (79) but conducting films are universally used (58).

VI. LITERATURE CITED

1. Alexander, J. M. and C. D. Coryell, Phys. Rev., 108, 1274 (1957).

2. Baerg, A. P. and R. M. Bartholomew, Can. J. Chem., 35, 980 (1957).

3. Banks, C. V., J. A. Thompson and J. W. O'Laughlin, Anal. Chem., 30, 1792 (1958).

4. Bayhurst, B. P., C. I. Browne, G. P. Ford, J. S. Gilmore, G. W. Knobeloch, E. J. Lang, M. A. Melnick and Carl Orth, Phys. Rev., 107, 325 (1957).

5. Bleuler, E. and G. J. Goldsmith. Experimental nucleonics. New York, Rinehart and Company, Inc. 1952.

6. Bohr, N. and J. A. Wheeler, Phys. Rev., 56, 426 (1939).

7. Bowles, B. J., F. Brown and J. P. Butler, Phys. Rev. 107, 751 (1957).

8. Cohen, B. L. and C. B. Fulmer, Nuclear Phys., 6, 547 (1958).

9. Coryell, C. D., Ann. Rev. Nuclear Sci., 2, 305 (1953).

10. Coryell, C. D. and N. Sugarman, eds. Radiochemical studies: the fission products. New York, McGraw-Hill Book Company, Inc. 1951.

11. Cowan, G. A., A. Turkevich, C. I. Browne and Los Alamos Radiochemistry Group, Phys. Rev., 122, 1286 (1961).

12. Crouthamel, C. E. and C. E. Johnson, Anal. Chem., 26, 1284 (1954).

13. Cunninghame, J. G., M. L. Sizeland, H. H. Willis, J. Eakins and E. R. Mercer, J. Inorg. and Nuclear Chem., 1, 163 (1955).

14. D'Agostino, O. and E. Segre, Gazz. chim. ital., 65, 1088 (1935). Original available but not translated; abstracted in Chem. Abstr., 30, 5117[9] (1936).

15. Duggan, E. L. and K. C. Smith, Science, 116, 305 (1952).

16. Faraggi, H., Ann. phys., 6, 325 (1951).

17. Fleming, W. H. Unpublished Ph.D. thesis. Hamilton, Ontario, McMaster University. 1954. Original not available; cited in Wanless, R. K. and H. G. Thode, Can. J. Phys., 33, 541 (1955).

18. Fleming, W. H., R. H. Tomlinson and H. G. Thode, Can. J. Phys., 32, 522 (1954).

19. Flerov, G. N., D. S. Klochkov, V. S. Skobin and V. V. Terent'ev, Soviet Phys.-"Doklady", 3, 79 (1958).

20. Fong, P. Phys. Rev., 122, 1542; 122, 1543; 122, 1545 (1956).

21. Ford, G. P. Nuclear charge distribution in U^{235} 14-mev. neutron fission. U. S. Atomic Energy Commission Report AECD-3597 [Technical Information Service Extension, AEC]. Washington, D. C., Office of Technical Services, U. S. Department of Commerce. 1953.

22. Foreman, B. M., Jr., W. M. Gibson, R. A. Glass and G. T. Seaborg, Phys. Rev., 116, 382 (1959).

23. Fowler, R. D. and R. W. Dodson, Phys. Rev., 55, 417 (1939).

24. Freiling, E. C. and L. R. Bunney, J. Am. Chem. Soc., 76, 1021 (1954).

25. Fritz, J. S., M. J. Richard, and W. Lane, Anal. Chem., 30, 1776 (1958).

26. Ghiorso, A. and Q. Van Winkle. Thermal-neutron fission properties of Pa^{231}, Th^{232} and Th^{230}. In L. I. Katzin, ed. Production and separation of U^{233}. U. S. Atomic Energy Commission Report TID-5223 [Technical Information Service Extension, AEC] pp. 593-4. Washington, D. C. Office of Technical Services, U. S. Department of Commerce. 1952.

27. Glendenin, L. E., Nucleonics, 2, No. 1, 12 (1948).

28. Glendenin, L. E., Phys. Rev., 75, 337 (1949).

29. Glendenin, L. E., E. P. Steinberg, M. G. Inghram and D. C. Hess, Phys. Rev., 84, 860 (1951).

30. Goeckermann, R. H. and I. Perlman, Phys. Rev., 76, 628 (1949).

31. Gunnink, R., L. J. Colby and J. W. Cobble, Anal. Chem., 31, 796 (1959).

32. Hahn, O. and L. Meitner, Naturwissenschaften, 23, 320 (1935).

33. Hahn, O. and L. Meitner, Naturwissenschaften, 27, 11 (1939).

34. Halpern, I., Ann. Rev. Nuclear Sci., 9, 245 (1959).

35. Harvey, B. G., Progr. in Nuclear Phys., 7, 89 (1959).

36. Heath, R. L. Scintillation gamma-ray catalogue. U. S. Atomic Energy Report IDO-16408 [Idaho Operations Office, AEC]. Washington, D. C., Office of Technical Services, U. S. Department of Commerce. 1957.

37. Hiller, D. M. Radiochemical studies on the photofission of thorium. Unpublished Ph.D. thesis. Ames, Iowa, Library, Iowa State University of Science and Technology. 1952.

38. Holland, L. Vacuum deposition of thin films. New York, N. Y., John Wiley and Sons, Inc. 1956.

39. Hughes, D. J. and R. B. Schwartz. Neutron cross sections. U. S. Atomic Energy Commission Report BNL-325, 2nd ed. [Brookhaven National Lab., Upton, N. Y.]. Washington, D. C., Office of Technical Services, U. S. Department of Commerce. 1958.

40. Inghram, M. G., Ann. Rev. Nuclear Sci., 4, 81 (1954).

41. Jackson, J. D., Can. J. Phys., 34, 767 (1956).

42. Jentschke, W. and F. Prankl, Naturwissenschaften, 27, 134 (1939).

43. Joliot, F., Compt. rend., 208, 341 (1939).

44. Jungerman, J. and S. C. Wright, Phys. Rev., 76, 1112 (1949).

45. Katcoff, S., Nucleonics, 16, No. 4, 78 (1958)

46. Keepin, G. R., T. F. Wimett and R. K. Zeigler, Phys. Rev., 107, 1044 (1957).

47. Kennett, T. J. and H. G. Thode, Can. J. Phys., 35, 969 (1957).

48. Kleinberg, J., ed. Collected radiochemical procedures. U. S. Atomic Energy Commission Report LA-1721, 2nd ed. [Los Alamos Scientific Lab., N. Mex.]. Washington, D. C., Office of Technical Services, U. S. Department of Commerce. 1958.

49. Koch, H. W., J. McElhinney and E. L. Gasteiger, Phys. Rev., 77, 329 (1950).

50. Kohman, T. P., Phys. Rev., 65, 63 (1944).

51. Korneev, E. I., V. S. Skobkin and G. N. Flerov, Soviet Phys. JETP, 10, 29 (1960).

52. Ladenburg, R., M. H. Kanner, H. Barschall and C. C. Van Voorhis, Phys. Rev., 56, 168 (1939).

53. Lavrukhina, A. K. and L. D. Krasavina, Soviet J. Atomic Energy, 2, 27 (1957).

54. Levy, H. B., H. G. Hicks, W. E. Nervik, P. C. Stevenson, J. B. Niday and J. C. Armstrong, Jr., Phys. Rev., 124, 544 (1961).

55. Lindner, M. and R. N. Osborne, Phys. Rev., 94, 1323 (1954).

56. Lindner, M. and R. N. Osborne, Phys. Rev., 103, 378 (1956).

57. MacNamara, J., C. B. Collins and H. G. Thode, Phys. Rev., 78, 129 (1950).

58. Mann, W. B. and H. H. Seliger, J. Research Natl. Bur. Standards, 50, 197 (1953).

59. Mayer, S. W. and E. C. Freiling, J. Am. Chem. Soc., 75, 5647 (1953).

60. McCorkle, W. H., Nucleonics, 15, No. 2, 91 (1957).

61. Meinke, W. W., ed. Chemical procedures used in bombardment work at Berkeley. U. S. Atomic Energy Commission Report AECD-2738 [Technical Information Service Extension, AEC]. Washington, D. C., Office of Technical Services, U. S. Department of Commerce. 1949.

62. Meitner, L., F. Strassmann and O. Hahn, Z. Physik, 109, 538 (1938).

63. Merrit, J. S., J. G. V. Taylor and P. J. Campion, Can. J. Chem., 37, 1109 (1959).

64. Meyer-Schützmeister, L. and D. G. Vincent, Z. Physik, 134, 9 (1952).

65. Miller, J. M. and J. Hudis, Ann. Rev. Nuclear Sci., 9, 159 (1959).

66. Nasuhoglu, R., S. Raboy, G. R. Ringo, L. E. Glendenin and E. P. Steinberg, Phys. Rev., 108, 1522 (1957).

67. Newson, H. W., Phys. Rev., 122, 1224 (1961).

68. Pappas, A. C. Radiochemical study of fission yields in the region of shell perturbations and the effect of closed shells in fission. U. S. Atomic Energy Commission Report AECU-2806 [Technical Information Service Extension, AEC]. Washington, D. C., Office of Technical Services, U. S. Department of Commerce. 1953.

69. Pate, B. D., Can. J. Chem., 36, 1707 (1958).

70. Pate, B. D., J. S. Foster and L. Yaffe, Can. J. Chem., 36, 1691 (1958).

71. Pate, B. D. and A. M. Poskanzer, Phys. Rev., 123, 647 (1961).

72. Pate, B. D. and L. Yaffe, Can. J. Chem., 33, 610 (1955).

73. Pate, B. D. and L. Yaffe, Can. J. Chem., 33, 929 (1955).

74. Pate, B. D. and L. Yaffe, Can. J. Chem., 34, 265 (1956).

75. Petruska, J. A., H. G. Thode and R. H. Tomlinson, Can. J. Phys., 33, 693 (1955).

76. Protopopov, A. N., M. I. Kuznetsov and E. G. Dermendzhiev, Soviet Phys. JETP, 11, 279 (1960).

77. Reactor handbook: physics. U. S. Atomic Energy Commission Report AECD-3645 [Technical Information Service Extension, AEC]. Washington, D. C., Office of Technical Services, U. S. Department of Commerce. 1955.

78. Roberts, R. B., R. C. Meyer and L. R. Hafstad, Phys. Rev., 55, 416 (1939).

79. Seliger, H. H. and L. Cavallo, J. Research Natl. Bur. Standards, 47, 41 (1951).

80. Serber, R., Phys. Rev., 72, 1114 (1947).

81. Stanley, C. W. and S. Katcoff, J. Chem. Phys., 17, 653 (1949).

82. Steinberg, E. P. and L. E. Glendenin. Survey of radiochemical studies of the fission process. In Proceedings of the International Conference on the peaceful uses of atomic energy, Geneva, 1955. Vol. 7, pp. 3-14. New York, United Nations. 1956.

83. Stensland, W. A. The radioactive decay of antimony-127. Unpublished M.S. thesis. Ames, Iowa, Library, Iowa State University of Science and Technology. 1961.

84. Strominger, D., J. M. Hollander and G. T. Seaborg, Revs. Modern Phys., 30, 585 (1958).

85. Sugihara, T. T., P. J. Drevinsky, E. J. Troianello and J. M. Alexander, Phys. Rev., 108, 1264 (1957).

86. Thode, H. G., Nucleonics, 3, No. 3, 14 (1948).

87. Thode, H. G., Trans. Roy. Soc. Can., Sect. 3, 45, 1 (1951).

88. Thode, H. G. and R. L. Graham, Can. J. Research, Sect. A, 25, 1 (1947).

89. Thomas, T. D., B. G. Harvey and G. T. Seaborg. Spallation fission competition in the heaviest elements. In Proceedings of the second United Nations International Conference on the peaceful uses of atomic energy, Geneva, 1958. Vol. 15, pp. 295-300. New York, United Nations. 1958.

90. Titterton, E. W., Phys. Rev., 83, 673 (1951).

91. Titterton, E. W., Phys. Rev., 83, 1076 (1951).

92. Titterton, E. W. and T. A. Brinkley, Phil. Mag., 41, 500 (1950).

93. Tsien, S.-T., Phys. Rev., 72, 1257 (1947).

94. Tsien, S.-T. and H. Faraggi, Compt. rend., 225, 294 (1947).

95. Tsien, S.-T., Z.-W. Ho, R. Chastel and L. Vigneron, J. phys. radium, 8, 165 (1947).

96. Turkevich, A. and J. B. Niday, Phys. Rev., 84, 52 (1951).

97. Turkevich, A., J. B. Niday and A. Tompkins, Phys. Rev., 89, 552 (1953).

98. Turner, L. A., Revs. Modern Phys., 12, 1 (1940).

99. Wade, W. H., J. Gonzalez-Vidal, R. A. Glass and G. T. Seaborg, Phys. Rev., 107, 1311 (1957).

100. Wahl, A. C., Phys. Rev., 99, 730 (1955).

101. Wanless, R. K. and H. G. Thode, Can. J. Phys., 33, 541 (1955).

102. Wetherill, G. W., Phys. Rev., 92, 907 (1953).

103. Wiles, D. R., B. W. Smith, R. Horsley and H. G. Thode, Can. J. Phys., 31, 419 (1953).

104. Wilson, R. R., Phys. Rev., 72, 189 (1947).

105. Zinn, W. H. Design and description of Argonne National Laboratory's Research Reactors (CP-3, CP-3', CP-5). In Proceedings of the International Conference on the peaceful uses of atomic energy, Geneva, 1955. Vol. 2, pp. 456-470. New York, United Nations. 1956.

106. Zumwalt, L. R. Absolute β-counting using end-window Geiger-Müller counters and experimental data on β-particle scattering effects. U. S. Atomic Energy Commission Report AECU-567 [Technical Information Service Extension, AEC]. Washington, D. C., Office of Technical Services, U. S. Department of Commerce. 1950.

VII. ACKNOWLEDGMENTS

The author thanks those who have assisted this investigation, especially Dr. Adolf F. Voigt for his efforts and encouragement and the Ames Laboratory of the Atomic Energy Commission for its funds and facilities.